N79-32574

NASA Contractor Report 159137

BEHAVIOR OF COMPOSITE BOLTED JOINTS AT
ELEVATED TEMPERATURE

Dale W. Wilson and R. Byron Pipes

UNIVERSITY OF DELAWARE
Center for Composite Materials
Newark, Delaware 19711

NASA Grant NSG-1409
September 1979

NASA
National Aeronautics and
Space Administration

Langley Research Center
Hampton, Virginia 23665

BEHAVIOR OF COMPOSITE BOLTED JOINTS AT ELEVATED TEMPERATURE

SUMMARY

Experimental results from an investigation which examines the combined effects of temperature, joint geometry and out-of-plane constraint upon the response of mechanically fastened composite joints are presented. Data are presented for simulated mechanically fastened joint conditions in two laminate configurations ($[0/\pm45/90]_{2s}$ and $[45/0/-45/0_2/-45/0/45/0_2/90]_s$) fabricated from Hercules AS/3501-6 graphite-epoxy. Strength and failure mode results are presented for the test temperatures of 21°C (70°F), 121°C (250°F) and 177°C (350°F) and for a range of the geometric parameters W/D and e/D from 3.71 to 7.43 and 1.85 to 3.69, respectively. A hole diameter, D of 5.16 mm (0.203 in.) was utilized for all tests. Pin bearing tests with out-of-plane constraint were conducted at room temperature only. All elevated temperature data were generated for pin bearing conditions. Three replicates of each test coupon geometry and laminate configuration were tested at each of three temperatures - totalling 126 tests in all. Ultrasonic "C" scan inspection of the failed specimens was employed to assess the damage region and to determine failure mode. Comparative data are presented for pin bearing and out-of-plane constraint conditions for the above mentioned joint configurations. The joint under pin loading was modeled by two-dimensional finite-element methods. Predicted net section strain concentrations were compared with experimental results.

TABLE OF CONTENTS

TABLE OF CONTENTS (Cont'd)

LIST OF TABLES

LIST OF FIGURES

NOMENCLATURE

Term	Description
edge distance (e)	Distance from center of hole to the end edge of the laminate.
hole diameter (D)	The diameter of the fastener hole.
width (W)	Width of the coupon which is equivalent to the half spacing between fasteners.
pin loading	Reacting the joint loads with a pin which offers no out-of-plane restraint.
out-of-plane constraint	Reacting the joint loads through the pin while constraining the out-of-plane deformations (deformations normal to plane of laminate).
bearing failure	A failure where localized crushing of the material reacting load leads to an elongation of the hole (see Fig. 4.91).
shear-out failure	Failure which is characterized by extensive cleavage damage parallel to the loading extending from the two sides of the fastener hole to the edge of the coupon (see Fig. 4.91).
net tension failure	Normal tensile failure occurring in the material adjacent to the fastener hole.
quasi-isotropic laminate	Laminate with the $[0/\pm45/90]_{2s}$ configuration.
bondable resistance temperature sensor	A strain insensitive resistive element which can be applied to the surface of a material to measure temperature.

Term	Description
0° dominated laminate	Referred to in this work as the laminate with the $[45/0/-45/0_2/-45/0/45/0_2/90]_s$ configuration.
ultrasonic "C" scan	A non-destructive inspection technique which uses ultrasonic waves to reveal information about the structure of the material.
gate	Electronic circuit used to selectively monitor a portion of the ultrasonic waveform.

1.0 INTRODUCTION

With increasing implementation of advanced composites in high technology aerospace applications, the understanding of bolted joint behavior remains a critical issue in the development of joining technology for composite materials. This is especially true for applications requiring high joint efficiency under extreme environmental conditions. Recent studies of bolted joint behavior have focused upon the development of analysis methods, the generation of design data, and the development of reinforcing techniques to improve joint strength [1-9].

Analytical studies have investigated the use of finite element methods to predict joint strength and determine failure modes in anistropic materials [10, 11] and the use of numerical techniques for analyzing elastically orthotropic cases by modified elasticity theory [3]. Most of the analytical work to date models the joint system as two-dimensional, but a few efforts have been made in three-dimensional analysis of joint behavior [12].

Most of the information required for designing bolted joints with boron-epoxy or graphite-epoxy composite materials at ambient conditions is available from the Air Force Design Guide [9]. The design guide provides design allowables for single-lap and double-lap joints with

moisture exposure are reported by Wilkins (8) and Kim and Whitney [4] for the 21°C (70°F), 121°C (250°F) range.

The reduction in laminate strength associated with bolt penetrations has stimulated attempts to reinforce the region around the penetration with various stiffening and softening materials in order to increase joint strength and to avoid the catastrophic net tension failure mode [6, 7]. The laminate stacking sequence effects observed by Quinn and Matthews [5] for quasi-isotropic glass-epoxy bolted joints are of more fundamental interest in understanding bolted joint behavior.

Only a sampling of the research on bolted joints has been reviewed here, but a review of the literature has revealed that there is a general lack of fundamental knowledge of the load transfer and failure mechanisms in composite bolted joints. The present work is intended to examine elevated temperature performance of graphite-epoxy composites in the 127°C (350°F) temperature region while taking a more fundamental look at the behavior observed. Groundwork is laid for use of ultrasonic "C" scan inspection of failed joints to evaluate damage patterns and modes.

Elevated temperature pin bearing strength and failure

mode data were generated for joint geometries with W/D ranging from 3.71 to 7.43 and e/D ranging from 1.85 to 3.69. Room temperature tests were conducted with out-of-plane constraint over a controlled contact area for comparison with pin bearing data. Ultrasonic "C" scan inspection techniques were used in evaluating damage zone nature and extent in the failed specimens. The results were tabulated for two laminate configurations, a 16 ply $[0/\pm45/90]_{2s}$ (quasi-isotropic) laminate and a 22 ply $[45/0/-45/0_2/-45/0/45/0_2/90]_s$ (0° dominated) laminate, fabricated from Hercules AS/3501-6 graphite epoxy prepreg.

2.0 EXPERIMENTAL PROCEDURE

2.1 Panel Fabrication

The laminates were fabricated from Hercules AS/3501-6 graphite-epoxy 30 cm. (12 inch) wide prepreg tape. All panels in the test program were made from the same batch of prepreg material to avoid any variability between panels due to batch differences. The panels were autoclave cured according to the standard procedures recommended for the AS/3501-6 system by Hercules Inc.

2.2 Test Coupon Fabrication

The test coupon geometry shown in Fig. 2.2.1 was fabricated for each bolted joint test. The test coupon was 15 cm. (6 inches) in length. Load is introduced through beveled end tabs bonded to the laminate and reacted by a pin through the hole located approximately fifteen hole diameters from the tabs. This single hole coupon configuration was designed to eliminate load history as a test variable by allowing only one test per coupon and provided uniform load introduction without interaction with the joint area. Glass-epoxy end tab material was used for the 21°C (70°F) and 121°C (250°F) tests while glass polyimide[1] material was used

---

[1]Glass polyimide material obtained from Howe Industries, Inc. was used due to future intent to test graphite-polyimide material at temperatures of 600°F.

for the 177°C (350°F) tests. Standard room temperature curing epoxy was used to bond the end tabs on the 21°C (70°F) test coupons and an elevated temperature epoxy (Eccobond 104) was used for bonding tabs to the elevated temperature coupons. Coupons were cut to widths of 1.905 cm. (0.750 in.), 2.540 cm. (1.000 in.) and 3.810 cm. (1.500 in.) using a precision diamond saw. Holes were drilled using a diamond core drill and then reamed to a 0.516 cm. (0.203 in.) diameter. Visual and ultrasonic inspection of the holes after machining revealed negligible machining damage. The holes were centered with respect to the specimen width and located either .953 cm. (0.375 in.) or 1.905 cm. (0.750 in.) from the end of the coupon. Dimensions of each sample were recorded prior to testing. Upon completion of fabrication, all test coupons were stored in sealed plastic bags containing a dessicant.

2.3 Fixture Design

Standard Instron friction grips were used for load introduction at the tab end of the coupon while a special clevis fixture shown in Figure 2.3.1 was designed to simulate the bolted load reaction through the hole. The "V" groove inserts were used in pin bearing tests and the load reacted by a high strength tungsten carbide steel pin. For out-of-plane constraint the inserts shown in Figure 2.3.2 were used,

where the washers were machined to constrain a known contact area of 0.65 cm. (0.100 in.^{2}) around the hole. The clevis fixture was mounted through a universal coupler to the load cell while friction grips were mounted on the crosshead. The fixture arrangement allowed a limited amount of self alignment capability.

2.4 Test Coupon Instrumentation

One test coupon for each geometry and test temperature was instrumented with strain gages to monitor far field, net section, shear-out, and bearing strains. These gages were located as shown in Figure 2.4.1. Elevated temperature adhesive (M Bond 610) was used for all strain gages in the elevated temperature test program. A resistance temperature sensor mounted on a dummy coupon was used to monitor test chamber temperature during testing.

Temperature compensation for the strain gages was achieved by balancing the bridge circuit manually after the gages had reached equilibrium with the constant test temperature. Chamber temperatures were constant during testing thus causing no further need for temperature compensation.

2.5 Test Methods and Procedures

Three replicates of each test coupon geometry and laminate were tested at each of the three temperatures -

totalling 126 tests in all. Tests were conducted within an environmental chamber providing temperature control over a -100°C to +325°C range. The test fixture was centered in the test chamber and all ports were sealed with insulation to assure a reasonably uniform chamber temperature. Temperature in close proximity to the test coupon was constantly monitored by the temperature gage mounted on the dummy sample. During all elevated temperature tests the coupon was "soaked" at temperature for 30 minutes to assure thermal equilibrium within the coupon during test.

Care was taken to align the test coupon in the grips and fixture so as not to introduce any eccentricities in load. Inspection of the grip marks on tested coupons revealed uniformity indicative of even load introduction. The tests were conducted with a crosshead speed of 0.05 cm/min. and the load versus crosshead displacement curve recorded for each test on the Instron x-y recorder. Failure load was determined as the maximum load attained before the load drop accompanying failure of the joint.

For pin bearing tests, clearance was left on each side of the laminate. The constraining washers were tightened finger tight for the out-of-plane constraint tests. The object was to simply inhibit out-of-plane deformation while applying minimal frictional load transfer. Strain data were

recorded at known load intervals for the instrumented tests. The far field strain gages were used to measure the effective longitudinal modulus of the laminates at the three test temperatures. The net section gage's strain output normalized by the far field strain was used to measure the strain concentration factor.

2.6 NDE of Failed Coupons

The failed coupons were subjected to ultrasonic "C" scan inspection and compared to the original "C" scans. While the undamaged regions compared identically, inspection of damage zone revealed information about the size and nature of damage inflicted at failure. All ultrasonic instrument settings were recorded. All coupons of the same laminate configuration were scanned under identical conditions to allow valid comparison of the damaged areas.

The "C" scan equipment is diagrammed in Figure 2.6.1 A wide band pulse of short duration is sent from a transducer through the specimen and the signal reflected from the specimen is received by the same transducer. This signal appears as a waveform shown in Figure 2.6.2 where the reflected signals from the front and back surfaces are characteristic of the material under test. In the peak amplitude "C" scan method, a gating circuit removes a specified portion of the waveform to be analyzed, usually the

back surface reflection. This gated portion of the waveform is then analyzed on a peak amplitude basis. The amplitude of the largest peak in the gated waveform is converted into a D. C. voltage which can be quantitized into 10 discrete regions. The recording amplifier then uses these discrete voltages to control the pen output which etches corresponding shades of grey on the recording paper.

Changes in thickness and delaminations cause changes in the waveform as shown in Figure 2.6.2. By adjusting the gate width and position it was possible to display delaminations as dark regions and changes in thickness as light regions. It should also be noted that the location of the delamination through the laminate thickness could be determined by examination of the waveform.

2.7 Data Analysis

A tabulation of data was compiled showing the sample dimensions, failure load, failure mode and the failure stresses (net tension, shear-out and bearing) and given in Appendix A. These stresses are simply the average stresses calculated using the following relationships.

$$F^{br} = P^{br}/(Dt) \qquad (1)$$

$$F^{so} = P^{so}/[2t(e-D/2)] \qquad (2)$$

$$F^{nt} = P^{nt}/((W-D)t) \qquad (3)$$

where F^{br}, F^{so} and F^{nt} are the failure stresses

P^{br}, P^{so} and P^{nt} are the failure loads.

3.0 RESULTS AND DISCUSSIONS

3.1 Comparison of Pinned and Out-of-Plane Constraint Loading Conditions

The results showing the effect of out-of-plane constraint on pin bearing strength are summarized in Figures 3.1.1 - 3.1.3. These figures show failure load as a function of W/D for the pin bearing loads with and without out-of-plane constraint while eliminating test temperature, laminate type, failure mode and e/D as variables. As shown in Figures 3.1.1 and 3.1.2 the quasi-isotropic laminate exhibited bearing failure in all cases with the out-of-plane constraint providing a 30-50% increase in strength. Over the range investigated, the pin bearing tests were relatively insensitive to W/D effects, while the out-of-plane constraint tests showed definite W/D dependence in the form of increased strength with increasing W/D.

The failure mode of the 0° dominated laminate with an e/D = 1.85 was shear-out and exhibited an 11% increase in strength with out-of-plane constraint. Both pin bearing and out-of-plane constraint tests exhibited decreasing strength with increasing W/D over the range of geometries investigated here as shown in Figure 3.1.3. These results suggest that

both the bearing and shear-out failure mechanisms are related to the out-of-plane deformation.

3.2 Effect of Test Temperature on Bolted Joint Strength

The effects of temperature on failure strength of bolted joints was investigated for pin bearing loading conditions only. The results are summarized for the two laminate configurations in Figures 3.2.1-3.2.4. In general, the strength diminished approximately 40% with a temperature increase from 21°C (70°F) to 177°C (350°F) for both laminate configurations. Figures 3.2.1 and 3.2.2 show failure load as a function of temperature for the quasi-isotropic laminate with e/D values of 1.85 and 3.69, respectively. It is apparent that W/D effects are insignificant for these cases. The test specimens with e/D of 1.85 were slightly more sensitive to temperature increases than the 3.69 geometry as indicated by a 50% decrease in strength with temperature for the e/D of 1.85 as compared to a 36% decrease for the e/D of 3.69.

The 0° dominated laminate results are presented in Figures 3.2.3 and 3.2.4. For this laminate the e/D effect on strength reduction with temperature is much less pronounced. An interesting result is the pronounced W/D effect for the e/D of 1.85 and little or no W/D effect for specimens of e/D 3.69. Examining the failed specimens it

was seen that the failure mode was predominantly shear-out for e/D of 1.85 while it was bearing for e/D of 3.69. Notice that for the 0° dominated laminate the difference in strength is very pronounced at 21°C (70°F), but decreases to an almost undetectible difference at 177°C (350°F).

3.3 The Effect of Temperature on Modulus

The effective initial longitudinal (E_x) modulus of the laminate was determined from the far field stress-strain curve on the instrumented samples and defined as average laminate stress/average far field strain. Summarized in Figures 3.3.1 and 3.3.2 are the variations of these experimentally determined modulus values with temperature. For the quasi-isotropic laminate, the modulus varied from 46.8 G Pa (6.8×10^6 psi) at 21°C (70°F) to 40.0 G Pa (5.8×10^6 psi) at 177°C (350°F). This translates to a 15% decrease in stiffness over the temperature interval. The 0° dominated laminate showed a similar 15% decrease in modulus (E_x) over the temperature interval with the room temperature modulus being 73.3 G Pa (11.5×10^6 psi) and the 177°C (350°F) modulus being 67.0 G Pa (9.7×10^6 psi). A significantly lower modulus was found for e/D = 1.85 geometry. The apparent change in effective longitudinal modulus can be attributed to strain gage position on the coupon. It is also believed that the large scatter in the data can be explained by small variations in the strain gage position. Finite element model

data shows that variations in the stress field around the hole extend beyond the 4.44 cm. (1-3/4 in.) location of the strain gage.

3.4 Evaluation of e/D Effects on Strength

When failure load as a function of e/D was investigated some interesting effects due to out-of-plane constraint and temperature became apparent. In Figure 3.4.1 failure load as a function of e/D for a quasi-isotropic laminate with out-of-plane constraint shows increasing strength with increasing e/D. The results for the same quasi-isotropic laminate tested in pin bearing without constraint are summarized in Figures 3.4.2-3.4.4. Considering the 21°C (70°F) cases only, it is apparent that strength decreases significantly with increases in e/D for pin bearing loading - the inverse of out-of-plane constraint results.

The strength dependence on e/D has been noted by Van Siclen [7] for a different set of loading conditions. Van Siclen's results show decreases in shear-out strength and increases in bearing strength with increasing e/D for double lap joints made from quasi-isotropic T300/PR286 graphite-epoxy. The present data demonstrate converse behavior for pin bearing tests for a quasi-isotropic laminate which failed in bearing. Bearing strength decreased for pinned tests while the imposition of out-of-plane constraint resulted in a duplication of Van Siclen's findings.

Insufficient data were available to fully characterize this behavior for the 0° dominated laminate due to a transition in failure mode from shear-out to bearing. Ignoring failure mode, the e/D dependent strength behavior exhibited by this system for pin bearing loading conditions was similar to the quasi-isotropic case. These results further substantiate the role of out-of-plane deformation in the bearing failure mechanism, while the implications for shear-out are not clear due to the change in failure mode for that data.

3.5 Evaluation of Combined e/D, W/D and Temperature Effects on Joint Strength

Results from the pin bearing tests of the quasi-isotropic laminate reveal a change in the load carrying ability with temperature. At 350°F the laminate failure load increases with e/D or for the W/D = 7.43 case remains unchanged. The 0° dominated laminate does not show this sensitivity to temperature as seen in Figures 3.5.1-3.5.3. There is an obvious W/D effect, however.

The region of the joint between the hole and the edge can be modelled simplistically as a short beam in bending (Fig. 3.5.4). The joint's strength in bearing is dependent upon the state of stress at the bearing surface (Point A) and the state of stress in that region is a function of the bending behavior. This was evident when finite element stress distributions and the strength data were analyzed for

values of e/D of 1.85 and 3.69. The larger bending deformation for the e/D of 1.85 geometry resulted in larger compressive stresses σ_y (as shown in Fig. 3.5.4) than for e/D of 3.69 coupons. Since the compressive stresses σ_x due to the pin load introduction were the same for both e/D values, the bending stresses σ_y were judged to be responsible for the differences in the state of stress at pin bearing location. The experimental results indicate that the geometric parameters e/D and W/D, as well as, out-of-plane constraint determine joint strength. Strength decreased with increasing values of e/D for pin bearing tests and increased with increasing e/D when out-of-plane constraint was imposed. This behavior varied with temperature for the quasi-isotropic laminate and while it was temperature insensitive for the 0° dominated laminate. W/D effects on the joint failure strength were also observed. The interaction of plate width, edge distance and temperature coupled with out-of-plane constraint conditions, determines the state of stress in the bearing zone ahead of the pin. The state of stress in this region in turn determines the strength of the joint.

3.6 Comparison of Experimental and Finite Element Modeled Net Section Strain Concentrations

Net section strain concentrations found experi-

mentally were compared with those determined from two-dimensional finite element models (3.6.1-3.6.2). The results are shown for 4 cases in tabular form in Table XVI. The correlation between the predicted and observed strain concentrations provided confidence that the model accurately predicted actual joint response.

3.7 Edge Deformation Predicted By Finite Element Model

After establishing a level of confidence in the finite element results, the model was used to examine joint in-plane deformations in the regions between the edge and the pin bearing surface of the hole. The deformations predicted for the two e/D cases are shown in Figure 3.7.1. The joint with an e/D = 2 (Figure 3.7.1) exhibits large deformations at the coupon free end and the deformations take on a bending configuration. The deformation of the specimen with e/D = 4 (Figure 3.7.1) does not exhibit bending characteristics and the magnitude of deformation is relatively small.

3.8 Bearing Stress Distribution Predicted By Finite Element Model

The finite element model was employed to predict bearing stress profiles ahead of the hole under pin bearing

loads. The results shown in Figures 3.8.1 and 3.8.2 indicate that the stress magnitudes are similar for both values of the e/D parameter. The model's prediction of similar bearing stress magnitudes for the two e/D values is not surprising. Regardless of e/D the coupon has the same bearing area. The difference in the strength for the two e/D values comes from the bending deformations discussed in section 3.7 and the associated change in the state of stress in front of the joint.

Predicted compressive stress concentrations for the e/D of 2.00 coupons were the same as those for the e/D of 4.00 coupons, thus verifying that the stress concentrations are not a factor in the e/D strength dependence. Differences in the σ_y stress magnitudes were observed and do verify that the state of stress in front of the joint is a factor in the pin bearing strength. The role of this state of stress in the failure mechanism is explained by the beam bending model in section 3.5. Important out-of-plane stress and deformation information could not be obtained from this two-dimensional model.

3.9 NDE of Damage Zone of Failed Coupons

Ultrasonic "C" scan inspection of the failed coupons produced the scans in Figures 3.9.2-3.9.6. These scans were used to assess the extent and type of damage at failure.

The ability to detect non-visible damage was found very useful in verifying the failure modes of coupons where visible damage was minimal. Figure 3.9.1 shows the three failure types encountered in this test program, bearing, shear-out and combination net-tension-shear-out.

Examples of the bearing failure "C" scans are shown in Figure 3.9.3. The hole elongation appears as an extension of the white region of the hole. The light grey regions ahead of the hole are characteristic of a change in thickness of the material and also some types of slight surface ply delaminations. The dark grey areas shown in Figure 3.9.3 are areas of severe delaminations and ply tear-outs. These characteristic patterns on the "C" scans were correlated visually with the types of damage described above for the failed specimens. All of the quasi-isotropic laminates shown in Figures 3.9.2 and 3.9.3 failed in bearing. Damage is localized with primary damage being an increase in thickness ahead of the loaded hole and very small areas of delamination (small dark areas) in the same region. The extent of damage did not change with temperature. The 0° dominated laminate exhibited bearing failure for all cases for e/D of 3.69 (Figure 3.9.5), but showed both bearing and shear-out failure for the e/D of 1.85 (Figure 3.9.4). Scans of the e/D 3.69 coupons show small damage areas similar to the quasi-isotropic case. Some delaminations can be seen

along the ±45° directions and again no changes in failure mode are seen with temperature. The e/D 1.85 scans show some interesting damage zone size effects. At room temperature the damage zone is a large region of severe delamination typical of a shear-out failure. At 121°C (250°F) the failure mode transitions from shear-out to predominantly bearing failure. At 177°C (350°F) the failure mode is again primarily shear-out. Notice that the damage extent is smaller and localized directly in front of the hole for the 177°C (350°F) samples. Scans of failed specimens tested with out-of-plane constraint shown in Figure 3.9.6 exhibit damage zones similar to those of pin bearing tests. The failure mode for the 0° dominated laminate with 3/D = 1.85 and W/D = 3.71 was a combination net section, tension shear-out failure mode when out-of-plane constraint was imposed, whereas the failure was shear-out for simple pin bearing.

3.10 Delayed Test Strength Degradation Phenomenon

Most of the instrumented samples were tested 150 days after laminate fabrication. The test results from these samples exhibited a significant decrease in strength as compared to the coupons tested under the same conditions 30 - 60 days after fabrication. The degradation in strength was evaluated by normalizing the residual strength of the 150 day coupons with respect to the average strength of the 30 - 60

day coupons tested under identical conditions. Figures 3.10.1 and 3.10.2 summarize the reduction in strength over the range of test temperatures explored. At 177°C (350°F) the effect was more pronounced than for the lower two test temperatures.

The processing, machining and testing histories for all test coupons were identical. Variability between panels was also ruled out as a cause since both the 150 day and 30 day test coupons were from the same set of panels and no strength variation between panels was detected in the previous tests. The moisture and thermal histories were the only differences between the two groups of test coupons. The instrumented test coupons were stored in sealed plastic bags containing desiccant for the 150 day period prior to test, but no moisture content measurements were taken. Each 121°C (250°F) and 177°C (350°F) instrumented test coupon underwent two thermal cycles to 163°C (325°F) in order to cure the elevated temperature adhesives for mounting the strain gages.

Results reported by Kim and Whitney [4] showed a decrease in strength of 10 percent due to moisture alone and no interaction between temperature and moisture could be ascertained. The present phenomena exhibits decreases in strength ranging from 11% to 50%. The effective decreases in strength show trends between 15% and 30% at the

21°C (70°F) and 121°C (250°F) temperatures and 30% to 40% decreases for the 177°C (350°F) tests. The strength reduction reported is significantly greater than 10%. This raises important questions about moisture and temperature effects on pin loaded composite joint strength.

4.0 CONCLUSIONS

Clamped tests (tests with controlled out-of-plane constraint) are much more useful than pinned tests from a design standpoint. A careful study of pinned and clamped tests with instrumentation monitoring the load and strain data in three dimensions would be very effective in clarifying bolted joint failure mechanisms.

In a comparison of strengths for pin bearing and out-of-plane constraint pin bearing loading conditions, the out-of-plane constraint was shown to increase the failure loads significantly for both bearing and shear-out failure modes. This finding implies a relationship between out-of-plane deformation and the bearing and shear-out failure mechanisms.

Increasing temperatures over the 21°C (70°F) to 177°C (350°F) range result in a decrease in pin bearing strength for the two laminates tested. This temperature dependent strength behavior is more pronounced for bearing failure than shear-out failure at lower temperatures, but both mechanisms exhibit similar behavior at temperatures approaching 177°C (350°F). Since the matrix is the temperature sensitive component of the system, the different temperature effects for the bearing and shear-out failure modes imply that the two modes are unique with respect to the matrix governed aspects of their failure mechanisms.

Laminate Young's modulus decreased with increasing temperature due to the change in matrix material properties with temperature. The reduction of stiffness with increased temperature allows increased laminate deformation for a given joint load level. The role of these deformations in the failure mechanism is explained next.

The net section strain concentrations predicted by a two-dimensional finite element model correllated well with experimentally measured values. Model-predicted deformations for the two e/D geometries, verified the presence of bending deformation ahead of the pin in the xy plane[1] for e/D of 1.85 while showing only extensional deformations for e/D of 3.69 as shown in Figure 3.7.1.

The effectiveness of ultrasonic "C" scan inspection of failed joints to evaluate damage size and type was demonstrated.

Results from the instrumented samples tested approximately 150 days after fabrication indicated a significant strength degradation when compared to test results at 30 - 60 days. Careful examination of the sample fabrication and test histories eliminated all test variables except moisture and thermal history. Insufficient data

[1]The xy plane is in the plane of the laminate with z being normal to the laminate.

were available to attribute the strength degradation phenomena to either of these variables. Results reported by Wilkins (8) and Kim and Whitney (4) indicate that moisture alone results in only a ten percent strength reduction at a given temperature. Since the magnitude of the strength reduction observed was significantly larger than that which might be attributed to moisture alone, the observed phenomena requires further study.

5.0 REFERENCES

1. Ashton, J.E., Burdouf, M.L., and Olson, F.O.; Design, Analysis and Testing Advanced Composite F-111 Fuselage. Convair/General Dynamics, SMD-059, 20 April 1971.

2. Hart-Smith, L.J.; Bolted Joints in Graphite-Epoxy Composites. Douglas Aircraft Company, NASA Contract Report NASA CR-144899, June 1976.

3. Jong, Theo de; "Stresses Around Pin-Loaded Holes in Elastically Orthotropic or Isotropic Plates", J. Composite Materials, Vol. 11, July 1977, p. 313.

4. Kim, R.Y. and Whitney, J.M., "Effect of Temperature and Moisture on Pin Bearing Strength of Composite Laminates", J. Composite Materials, Vol. 10, April 1976, p. 149.

5. Quinn, W.J. and Matthews, F.L., "The Effect of Stacking Sequence on the Pin-Bearing Strength in Glass Fibre Reinforced Plastic", J. Composite Materials, Vol. 11, April 1977, p. 139.

6. Padawer, G.E., "The Strength of Bolted Connections in Graphite/Epoxy Composites Reinforced by Colaminated Boron Film", Composite Material: Testing and Design (Second Conference), ASTM STP 497, American Society for Testing and Materials, 1972, pp. 396-414.

7. Van Siclen, R.C.: "Evaluation of Bolted Joints in Graphite-Epoxy," Proceedings of the Army Symposium on Solid Mechanics, AMMRC MS74-8, September 1974.

8. Wilkins, D.J., "Environmental Sensitivity Tests of Graphite-Epoxy Bolt Bearing Properties," Composite Materials: Testing and Design (Fourth Conference) ASTM STP 617, American Society for Testing and Materials, 1977, pp. 497-513.

9. Advanced Composites Design Guide, Vol. I, Design, Third Edition, Contract F33615-74-C-5075, North American Rockwell/Los Angeles Division, January 1973.

10. Waszczak, J.P. and Cruse, T.A., "Failure Mode and Strength Predictions of Anisotropic Bolt Bearing Specimens", J. of Composite Materials, Vol. 5, July 1971, p. 421.

11. Waszczak, J.P. and Cruse, T.A., "A Synthesis Procedure for Mechanically Fastened Joints in Advanced Composite Materials", AIAA/ASME/SAE 14th Structures, Structural Dynamics, and Materials Conference, March 1973.

12. Harris, H.G. and Ojalvo, I.U.: "Simplified Three-Dimensional Analysis of Mechanically Fastened Joints", Proceedings of the Army Symposium on Solid Mechanics, AMMRC MS74-8, September 1974.

6.0 ACKNOWLEDGEMENTS

The authors would like to recognize David A. Riegner for his contribution in the development of the finite element models of the two bolted joint configurations.

7.0 APPENDIX A (Data Tables)

TABLE I A

$[45/0/-45/0_2/-45/0/45/0_2/90]_s$ BOLTED JOINT STRENGTH DATA

TEST TEMP. = 70°F

English Units

Sample	e/D	T (in.)	W (in.)	Pin Dia. (in.)	Failure Load (lb_f)	Bearing Stress (10^4PSI)	Shear Stress (10^4PSI)	Net Tension Stress (10^4PSI)	Mode
02C2B	3.69	0.117	0.998	0.202	1996	8.45	0.24	2.14	B
01R2B	3.69	0.117	0.997	0.202	2073	8.86	0.25	2.23	B
02C2T	3.69	0.118	0.999	0.202	1974	8.28	0.24	2.10	B
01C1B	3.69	0.118	1.497	0.202	2062	8.65	0.25	1.35	B
02R1B	3.69	0.117	1.498	0.202	1941	8.21	0.24	1.28	B
01R1B	3.69	0.116	1.508	0.202	1720	7.22	0.21	1.14	B
01C3B	3.69	0.122	0.747	0.202	1985	8.10	0.23	2.99	B
01R3B	3.69	0.114	0.747	0.202	1897	8.23	0.24	3.05	B
02C3B	3.69	0.119	0.748	0.202	1776	7.39	0.21	2.73	B

TABLE 1 B

$[45/0/-45/0_2/-45/0/45/0_2/90]_s$ BOLTED JOINT STRENGTH DATA

TEST TEMP. = 70°F (21°C)

S.I. Units

Sample	e/D	T (cm.)	W (cm.)	Pin Dia. (cm.)	Failure Load (Newtons)	Bearing Stress M Pa	Shear Stress M Pa	Net Tension Stress M Pa	Mode
02C2B	3.69	0.297	2.535	0.511	88.82	582.8	16.6	147.6	B
01R2B	3.69	0.297	2.532	0.511	92.25	611.1	17.2	153.8	B
02C2T	3.69	0.300	2.537	0.511	87.84	571.1	16.6	144.8	B
01C1B	3.69	0.300	3.802	0.511	91.76	596.6	17.2	93.1	B
02R1B	3.69	0.297	3.805	0.511	86.37	566.2	16.6	88.3	B
01R1B	3.69	0.295	3.830	0.511	76.54	498.0	14.5	78.6	B
01C3B	3.69	0.310	1.897	0.511	88.33	558.7	15.9	206.2	B
01R3R	3.69	0.290	1.897	0.511	84.42	567.6	16.6	210.4	B
02C3B	3.69	0.302	1.900	0.511	79.03	509.7	14.5	183.3	B

TABLE II A

$[45/0/-45/0_2/-45/0/45/0_2/90]_s$ BOLTED JOINT STRENGTH DATA

TEST TEMP. = 70°F

English Units

Sample	e/D	T (in.)	W (in.)	Pin Dia. (in.)	Failure Load (lb_f)	Bearing Stress (10^4PSI)	Shear Stress (10^4PSI)	Net Tension Stress (10^4PSI)	Mode
01L3T	1.85	0.115	0.745	0.202	2106	9.06	0.61	3.37	S
01C3T	1.85	0.120	0.747	0.202	2205	9.10	0.61	3.37	S
01L3B*	1.85	0.117	0.744	0.202	1776	7.51	0.51	2.80	S
01L2B	1.85	0.121	0.996	0.202	2128	8.71	0.59	2.21	S
01L2T	1.85	0.117	0.996	0.202	2117	8.96	0.60	2.28	S
01C2T*	1.85	0.120	0.997	0.202	1654	6.82	0.46	1.73	S
02L1B	1.85	0.116	1.498	0.202	1808	7.72	0.52	1.20	S
02L1T	1.85	0.115	1.499	0.202	1919	8.26	0.56	1.29	S
02R1T*	1.85	0.118	1.498	0.202	1786	7.49	0.51	1.17	S

*Indicates tests after 4 month storage.

TABLE II B

$[45/0/-45/0_2/-45/0/45/0_2/90]_s$ BOLTED JOINT STRENGTH DATA

TEST TEMP. = 70°F (21°C)

S.I. Units

Sample	e/D	T (cm.)	W (cm.)	Pin Dia. (cm.)	Failure Load (Newtons)	Bearing Stress M Pa	Shear Stress M Pa	Net Tension Stress M Pa	Mode
01L3T	1.85	0.292	1.892	0.511	9372	624.9	42.1	232.4	S
01C3T	1.85	0.305	1.897	0.511	9812	627.6	42.1	232.4	S
01L3B	1.85	0.297	1.890	0.511	7903	518.0	35.2	193.1	S
01L2B	1.85	0.307	2.530	0.511	9470	600.7	40.7	152.4	S
01L2T	1.85	0.297	2.530	0.511	9421	618.0	41.4	157.3	S
01C2T	1.85	0.305	2.532	0.511	7360	470.4	31.7	119.3	S
02L1B	1.85	0.295	3.805	0.511	8046	532.4	35.9	82.8	S
02L1T	1.85	0.292	3.807	0.511	8540	569.7	38.6	89.0	S
02R1T	1.85	0.300	3.805	0.511	7948	516.6	35.2	80.7	S

TABLE III A

$[45/0/-45/0_2/-45/0/45/0_2/90]_s$ BOLTED JOINT STRENGTH DATA

TEST TEMP. = 250°F

English Units

Sample	e/D	T (in.)	W (in.)	Pin Dia. (in.)	Failure Load (lb_f)	Bearing Stress (10^4PSI)	Shear Stress (10^4PSI)	Net Tension Stress (10^4PSI)	Mode
02R3B	3.69	0.115	0.748	0.202	1535	6.61	0.19	2.45	B
01R3T	3.69	0.114	0.747	0.202	1471	6.38	0.18	2.37	B
04L2B*	3.69	0.125	0.754	0.202	1015	4.02	0.12	1.47	B
01C2B	3.69	0.121	0.996	0.202	1535	6.28	0.18	1.60	B
02L2B	3.69	0.116	0.998	0.202	1511	6.44	0.19	1.64	B
04R2B*	3.69	0.128	1.002	0.202	1352	5.23	0.15	1.32	B
01R1T	3.69	0.117	1.502	0.202	1495	6.33	0.18	0.98	B
02C1T	3.69	0.122	1.505	0.202	1522	6.18	0.18	0.96	B
04C2B*	3.69	0.129	1.505	0.202	1301	4.99	0.14	0.77	B

*Indicates test after 4 month storage.

TABLE III B

$[45/0/-45/0_2/-45/0/45/0_2/90]_s$ BOLTED JOINT STRENGTH DATA

TEST TEMP. = 121°C (250°F)

S.I. Units

Sample	e/D	T (cm.)	W (cm.)	Pin Dia. (cm.)	Failure Load (Newtons)	Bearing Stress M Pa	Shear Stress M Pa	Net Tension Stress M Pa	Mode
02R3B	3.69	0.292	1.900	0.511	6831	455.9	13.1	169.0	B
01R3T	3.69	0.290	1.897	0.511	6546	440.0	12.4	163.5	B
04L2B	3.69	0.318	1.915	0.511	4517	277.3	8.3	108.3	B
01C2B	3.69	0.307	2.530	0.511	6831	433.1	12.4	110.4	B
02L2B	3.69	0.295	2.535	0.511	6724	444.2	13.1	113.1	B
04R2B	3.69	0.325	2.545	0.511	6016	360.7	10.3	91.0	B
01R1T	3.69	0.297	3.815	0.511	6653	436.6	12.4	67.6	B
02C1T	3.69	0.310	3.823	0.511	6773	426.2	12.4	66.2	B
04C2B	3.69	0.328	3.823	0.511	5789	344.2	9.7	53.1	B

TABLE IV A

$[45/0/-45/0_2/-45/0/45/0_2/90]_s$ BOLTED JOINT STRENGTH DATA

TEST TEMP. = 250°F

English Units

Sample	e/D	T (in.)	W (in.)	Pin Dia. (in.)	Failure Load (lb_f)	Bearing Stress (10^4PSI)	Shear Stress (10^4PSI)	Net Tension Stress (10^4PSI)	Mode
02R2T	1.85	0.118	0.997	.202	1610	6.75	0.46	1.72	S
02L2T	1.85	0.115	0.997	.202	1654	7.12	0.48	1.81	B
04R1T*	1.85	0.129	1.000	.202	1433	5.50	0.37	1.39	B
02L4B	1.85	0.116	0.739	.202	1720	7.34	0.49	2.76	S
01C4T	1.85	0.120	0.747	.202	1643	6.78	0.46	2.51	B
02L4T*	1.85	0.116	0.745	.202	1378	5.88	0.40	2.19	B
01C1T	1.85	0.118	1.499	.202	1522	6.38	0.43	0.99	B
01L1T	1.85	0.120	1.501	.202	1467	6.05	0.41	0.94	B
01L1B*	1.85	0.121	1.501	.202	1390	5.69	0.38	0.88	B

*Indicates tests after 4 month storage.

TABLE IV B

$[45/0/-45/0_2/-45/0/45/0_2/90]_s$ BOLTED JOINT STRENGTH DATA

TEST TEMP. = 121°C (250°F)

S.I. Units

Sample	e/D	T (cm.)	W (cm.)	Pin Dia. (cm.)	Failure Load (Newtons)	Bearing Stress M Pa	Shear Stress M Pa	Net Tension Stress M Pa	Mode
02R2T	1.85	0.300	2.532	0.511	7165	465.5	31.7	118.6	S
02L2T	1.85	0.292	2.532	0.511	7360	491.1	33.1	124.8	B
04R1T	1.85	0.328	2.540	0.511	6377	379.3	25.5	95.9	B
02L4B	1.85	0.295	1.877	0.511	7654	506.2	33.8	190.4	S
01C4T	1.85	0.305	1.897	0.511	7311	467.6	31.7	173.1	B
02L4T	1.85	0.295	1.892	0.511	6132	405.5	27.6	151.0	B
01C1T	1.85	0.300	3.807	0.511	6773	440.0	29.7	68.3	B
01L1T	1.85	0.305	3.813	0.511	6528	417.3	28.3	64.8	B
01L1B	1.85	0.307	3.813	0.511	6186	392.4	26.2	60.7	B

TABLE V A

$[45/0/-45/0_2/-45/0/45/0_2/90]_s$ BOLTED JOINT STRENGTH DATA

TEST TEMP. = 350°F

English Units

Sample	e/D	T (in.)	W (in.)	Pin Dia. (in.)	Failure Load (lb_f)	Bearing Stress (10^4PSI)	Shear Stress (10^4PSI)	Net Tension Stress (10^4PSI)	Mode
05R3T	3.69	0.119	0.752	0.202	1169	4.86	0.14	1.79	B
05R3B	3.69	0.122	0.752	0.202	1102	4.47	0.13	1.64	B
05L3T*	3.69	0.119	0.753	0.202	860	3.58	0.10	1.31	B
05R2T	3.69	0.119	1.001	0.202	1147	4.77	0.14	1.21	B
05L4B	3.69	0.119	1.004	0.202	1171	4.87	0.14	1.23	B
05R2B*	3.69	0.121	1.001	0.202	717	2.93	0.08	0.74	B
05L1B	3.69	0.120	1.500	0.202	1103	4.55	0.13	0.70	B
05C1B	3.69	0.123	1.498	0.202	1202	4.84	0.14	0.75	B
05L1T*	3.69	0.118	1.500	0.202	750	3.15	0.09	0.49	B

Indicates test after 4 month storage.

TABLE V B

$[45/0/-45/0_2/-45/0/45/0_2/90]_s$ BOLTED JOINT STRENGTH DATA

TEST TEMP. = 350°F (177°C)

S.I. Units

Sample	e/D	T (cm.)	W (cm.)	Pin Dia. (cm.)	Failure Load (Newtons)	Bearing Stress M Pa	Shear Stress M Pa	Net Tension Stress M Pa	Mode
05R3T	3.69	0.302	1.910	0.511	5202	335.2	9.7	123.5	B
05R3B	3.69	0.310	1.910	0.511	4904	308.3	9.0	113.1	B
05L3T	3.69	0.302	1.913	0.511	3827	246.9	6.9	90.4	B
05R2T	3.69	0.302	2.543	0.511	5704	329.0	9.7	83.5	B
05L4B	3.69	0.302	2.550	0.511	5211	335.9	9.7	84.8	B
05R2B	3.69	0.307	2.543	0.511	3191	202.1	5.5	51.0	B
05L1B	3.69	0.305	3.810	0.511	4908	313.8	9.0	48.3	B
05C1B	3.69	0.312	3.805	0.511	5349	333.8	9.7	51.7	B
05L1T	3.69	0.300	3.810	0.511	3338	217.3	6.2	33.8	B

TABLE VI A

$[45/0/-45/0_2/-45/0/45/0_2/90]_s$ BOLTED JOINT STRENGTH DATA

TEST TEMP. = 350°F

English Units

Sample	e/D	T (in.)	W (in.)	Pin Dia. (in.)	Failure Load (lb_f)	Bearing Stress (10^4PSI)	Shear Stress (10^4PSI)	Net Tension Stress (10^4PSI)	Mode
05R4B	1.85	0.121	0.748	.202	1257	5.14	0.35	1.90	B
05L3B	1.85	0.119	0.752	.202	1301	5.28	0.36	1.99	S/B
05L2T*	1.85	0.122	0.753	.202	860	3.49	0.24	1.28	S/B
05C3T	1.85	0.127	1.002	.202	1257	4.90	0.33	1.24	S/B
05R1T	1.85	0.125	0.998	.202	1279	5.07	0.34	1.29	S/B
05L4T*	1.85	0.120	1.005	.202	871	3.59	0.24	0.90	B
05C2T	1.85	0.126	1.505	.202	1235	4.85	0.32	0.75	S/B
05C2B	1.85	0.126	1.505	.202	1235	4.85	0.32	0.75	S/B
05C1T*	1.85	0.122	1.495	.202	915	3.71	0.25	0.58	S/B

*Indicates tests after 4 month storage.

TABLE VI B

$[45/0/-45/0_2/-45/0/45/0_2/90]_s$ BOLTED JOINT STRENGTH DATA

TEST TEMP. = 350°F (177°C)

S.I. Units

Sample	e/D	T (cm.)	W (cm.)	Pin Dia. (cm.)	Failure Load (Newtons)	Bearing Stress M Pa	Shear Stress M Pa	Net Tension Stress M Pa	Mode
05R4B	1.85	0.307	1.900	0.511	5594	354.5	24.1	131.0	B
05L3B	1.85	0.302	1.910	0.511	5789	364.2	24.8	137.3	S/B
05L2T	1.85	0.310	1.913	0.511	3827	240.7	16.6	88.3	S/B
05C3T	1.85	0.323	2.545	0.511	5594	338.0	22.8	85.5	S/B
05R1T	1.85	0.318	2.535	0.511	5692	349.7	23.4	89.0	S/B
05L4T	1.85	0.305	2.553	0.511	3876	247.6	16.6	62.1	B
05C2T	1.85	0.320	3.823	0.511	5496	334.5	22.1	51.7	S/B
05C2B	1.85	0.320	3.823	0.511	5496	334.5	22.1	51.7	S/B
05C1T	1.85	0.122	3.797	0.511	4072	255.9	17.2	40.0	S/B

TABLE VII A

$[0/\pm45/90]_{2s}$ BOLTED JOINT STRENGTH DATA

TEST TEMP. = 70°F

English Units

Sample	e/D	T (in.)	W (in.)	Pin Dia. (in.)	Failure Load (lb_f)	Bearing Stress (10^4PSI)	Shearout Stress (10^4PSI)	Net Tension Stress (10^4PSI)	Mode
44C2B	3.69	.092	.997	.201	1213	6.56	0.19	1.66	B
44C3B	3.69	.092	.997	.201	1279	6.92	0.20	1.75	B
44C3T	3.69	.090	.996	.201	891	4.81	0.14	1.25	B
44C1B	3.69	.090	1.500	.201	1213	6.71	0.19	1.04	B
46L1B	3.69	.088	1.499	.201	1279	7.23	0.21	1.12	B
46L1T	3.69	.089	1.501	.201	1213	6.78	0.19	1.05	B
44R4B	3.69	.089	.748	.201	1191	6.66	0.19	2.45	B
44R4T	3.69	.088	.748	.201	1213	6.85	0.20	2.52	B
44R3T	3.69	.089	.747	.201	1191	6.66	0.19	2.45	B

TABLE VII B

$[0/\pm45/90]_{2s}$ BOLTED JOINT STRENGTH DATA

TEST TEMP. = 21°C (70°F)

S.I. Units

Sample	e/D	T (cm.)	W (cm.)	Pin Dia. (cm.)	Failure Load (Newtons)	Bearing Stress M Pa	Shear Stress M Pa	Net Tension Stress M Pa	Mode
44C2B	3.69	0.234	2.532	0.511	5398	452.5	13.0	114.5	B
44C3B	3.69	0.234	2.532	0.511	5692	477.3	13.8	120.7	B
44C3T	3.69	0.229	2.530	0.511	3965	331.7	9.7	86.2	B
44C1B	3.69	0.229	3.810	0.511	5398	462.8	13.1	77.3	B
46L1B	3.69	0.224	3.807	0.511	5692	498.7	14.5	72.4	B
46L1T	3.69	0.226	3.813	0.511	5398	467.6	13.1	90.4	B
44R4B	3.69	0.226	1.900	0.511	5300	459.3	13.1	169.0	B
44R4T	3.69	0.224	1.900	0.511	5398	472.4	13.8	173.8	B
44R3T	3.69	0.226	1.897	0.511	5300	459.3	13.1	168.9	B

TABLE VIII A

$[0/\pm45/90]_{2s}$ BOLTED JOINT STRENGTH DATA

TEST TEMP. = 70°F

English Units

Sample	e/D	T (in.)	W (in.)	Pin Dia. (in.)	Failure Load (lb_f)	Bearing Stress (10^4PSI)	Shear Stress (10^4PSI)	Net Tension Stress (10^4PSI)	Mode
45L3T	1.85	0.088	0.748	.202	1356	7.63	0.51	2.82	B
45L3B	1.85	0.089	0.751	.202	1478	8.22	0.55	3.02	B
44R3B*	1.85	0.089	0.747	.202	1169	6.50	0.44	2.41	B
44C2T	1.85	0.091	0.997	.202	1434	7.80	0.53	1.98	B
44L2B	1.85	0.088	0.996	.202	1356	7.63	0.51	1.94	B
44L2T*	1.85	0.089	0.996	.202	1136	6.30	0.51	1.92	B
44L1B	1.85	0.090	1.499	.202	1389	7.56	0.51	1.19	B
44L1T	1.85	0.090	1.500	.202	1434	7.89	0.53	1.23	B
44R1T*	1.85	0.089	1.503	.202	1257	6.99	0.47	1.09	B

*Indicate test took place after 4 month storage.

TABLE VIII B

$[0/\pm45/90]_{2s}$ BOLTED JOINT STRENGTH DATA

TEST TEMP. = 21°C (70°F)

S.I. Units

Sample	e/D	T (cm.)	W (cm.)	Pin Dia. (cm.)	Failure Load (Newtons)	Bearing Stress M Pa	Shear Stress M Pa	Net Tension Stress M Pa	Mode
45L3T	1.85	0.224	1.900	0.511	6034	562.2	35.2	194.5	B
45C3B	1.85	0.226	1.908	0.511	6577	566.9	37.9	208.3	B
44R3B	1.85	0.226	1.897	0.511	5202	448.3	30.3	166.2	B
44C2T	1.85	0.231	2.532	0.511	6381	538.0	36.6	136.6	B
44L2B	1.85	0.224	2.530	0.511	6034	526.2	35.2	133.8	B
44L2T	1.85	0.226	2.530	0.511	5055	434.5	35.2	132.4	B
44L1B	1.85	0.229	3.807	0.511	6181	521.4	35.2	82.1	B
44L1T	1.85	0.229	3.810	0.511	6381	544.2	36.6	84.8	B
44R1T	1.85	0.226	3.818	0.511	5594	482.1	32.4	75.2	B

TABLE IX A

$[0/\pm45/90]_{2s}$ BOLTED JOINT STRENGTH DATA

TEST TEMP. - 250°F

English Units

Sample	e/D	T (in.)	W (in.)	Pin Dia. (in.)	Failure Load (lb_f)	Bearing Stress (10^4PSI)	Shearout Stress (10^4PSI)	Net Tension Stress (10^4PSI)	Mode
45R2B	3.69	.088	.996	.201	915	4.95	0.15	1.31	B
46L3T	3.69	.090	1.000	.201	1058	5.80	0.17	1.47	B
46L3B	3.69	.090	.999	.201	1021	5.65	0.16	1.42	B
46L4B	3.69	.091	.749	.201	1003	5.48	0.16	2.01	B
46C3T	3.69	.089	.755	.201	970	5.43	0.16	1.97	B
46L4T	3.69	.090	.750	.201	1032	5.70	0.16	2.09	B
46L2T	3.69	.090	1.500	.201	992	5.48	0.16	0.85	B
45R1B	3.69	.089	1.504	.201	1047	5.85	0.17	0.90	B
45R1T	3.69	.087	1.502	.201	948	5.42	0.16	0.84	B

TABLE IX B

$[0/\pm45/90]_{2s}$ BOLTED JOINT STRENGTH DATA

TEST TEMP. = 121°C (250°F)

S.I. Units

Sample	e/D	T (cm.)	W (cm.)	Pin Dia. (cm.)	Failure Load (Newtons)	Bearing Stress M Pa	Shear Stress M Pa	Net Tension Stress M Pa	Mode
45R2B	3.69	0.224	2.530	0.511	4072	341.4	10.3	90.4	B
46L3T	3.69	0.229	2.540	0.511	4708	400.0	11.7	101.4	B
46L3B	3.69	0.229	2.537	0.511	4543	389.7	11.0	97.9	B
46L4B	3.69	0.231	1.902	0.511	4463	378.0	11.0	138.6	B
46C3T	3.69	0.226	1.918	0.511	4317	374.5	11.0	135.9	B
46L4T	3.69	0.229	1.905	0.511	4592	393.1	11.0	144.1	B
46L2T	3.69	0.229	3.810	0.511	4414	378.0	11.0	58.6	B
45R1B	3.69	0.226	3.820	0.511	4659	403.5	11.7	62.1	B
45R1T	3.69	0.221	3.815	0.511	4219	373.8	11.0	57.9	B

TABLE X A

$[0/\pm45/90]_{2s}$ BOLTED JOINT STRENGTH DATA

TEST TEMP. - 250°F

English Units

Sample	e/D	T (in.)	W (in.)	Pin Dia. (in.)	Failure Load (lb_f)	Bearing Stress (10^4PSI)	Shear Stress (10^4PSI)	Net Tension Stress (10^4PSI)	Mode
45L4T	1.85	0.088	0.746	.202	1059	5.96	0.40	2.21	B
45L4B	1.85	0.088	0.749	.202	1036	5.83	0.39	2.15	B
45C4T*	1.85	0.090	0.751	.202	905	4.98	0.34	1.83	B
45L2T	1.85	0.088	0.997	.202	1103	6.20	0.42	1.58	B
45L2B	1.85	0.088	0.978	.202	1092	6.14	0.41	1.56	B
44R2B*	1.85	0.090	0.998	.202	889	4.89	0.33	1.24	B
45L1T	1.85	0.089	1.496	.202	1014	5.64	0.38	0.89	B
44L3B	1.85	0.088	1.499	.202	1014	5.70	0.38	0.83	B
44L3T*	1.85	0.089	1.499	.202	785	4.37	0.29	0.68	B

*Indicates test after 4 month storage.

TABLE X B

$[0/\pm45/90]_{2s}$ BOLTED JOINT STRENGTH DATA

TEST TEMP. = 121°C (250°F)

S.I. Units

Sample	e/D	T (cm.)	W (cm.)	Pin Dia. (cm.)	Failure Load (Newtons)	Bearing Stress M Pa	Shear Stress M Pa	Net Tension Stress M Pa	Mode
45L4T	1.85	0.224	1.895	0.511	4712	411.1	27.6	152.4	B
45L4B	1.85	0.224	1.902	0.511	4610	402.1	26.9	148.3	B
45C4T	1.85	0.229	1.908	0.511	4027	343.5	23.4	126.2	B
45L2T	1.85	0.224	2.532	0.511	4908	427.6	29.0	109.0	B
45L2B	1.85	0.224	2.535	0.511	4859	423.5	28.3	107.6	B
44R2B	1.85	0.229	2.535	0.511	3956	337.3	22.8	85.5	B
45L1T	1.85	0.226	3.800	0.511	4512	389.0	26.2	61.4	B
44L3B	1.85	0.224	3.807	0.511	4512	393.1	26.2	61.4	B
44L3T	1.85	0.226	3.807	0.511	3493	301.4	20.2	46.9	B

TABLE XI A

$[0/\pm45/90]_{2s}$ BOLTED JOINT STRENGTH DATA

TEST TEMP. = 350°F

English Units

Sample	e/D	T (in.)	W (in.)	Pin Dia. (in.)	Failure Load (lb_f)	Bearing Stress (10^4PSI)	Shear Stress (10^4PSI)	Net Tension Stress (10^4PSI)	Mode
47C3T	3.69	.091	0.753	.202	810	4.41	0.13	1.61	B
47L3T	3.69	.089	0.752	.202	849	4.72	0.14	1.73	B
47C4T*	3.69	.089	0.755	.202	348	1.94	0.06	0.71	B
47R3B	3.69	.090	1.004	.202	838	4.61	0.13	1.16	B
47C1T	3.69	.092	0.999	.202	882	4.74	0.14	1.20	B
47C2T*	3.69	.091	1.002	.202	518	2.82	0.08	0.71	B
47R2B	3.69	.091	1.495	.202	783	4.26	0.12	0.67	B
47L1T	3.69	.089	1.503	.202	728	4.05	0.12	0.63	B
47R1B*	3.69	.089	1.496	.202	650	3.62	0.10	0.56	B

*Indicates sample was tested after 4 month storage.

TABLE XI B

$[0/\pm 45/90]_{2s}$ BOLTED JOINT STRENGTH DATA

TEST TEMP. = 177°C (350°F)

S.I. Units

Sample	e/D	T (cm.)	W (cm.)	Pin Dia. (cm.)	Failure Load (Newtons)	Bearing Stress M Pa	Shear Stress M Pa	Net Tension Stress M Pa	Mode
47C3T	3.69	0.231	1.913	0.511	3605	304.2	9.0	111.0	B
47L3T	3.69	0.226	1.910	0.511	3778	325.5	9.7	119.3	B
47C4T	3.69	0.226	1.918	0.511	1549	133.8	4.1	49.0	B
47R3B	3.69	0.229	2.550	0.511	3729	318.0	9.0	80.0	B
47C1T	3.69	0.234	2.537	0.511	3925	326.9	9.7	82.8	B
47C2T	3.69	0.231	2.545	0.511	2305	195.9	5.5	49.0	B
47R2B	3.69	0.231	3.797	0.511	3484	293.8	8.3	46.2	B
47L1T	3.69	0.226	3.818	0.511	3240	279.3	8.3	43.5	B
47R1B	3.69	0.226	3.800	0.511	2893	249.7	6.9	38.6	B

TABLE XII A

$[0/\pm45/90]_{2s}$ BOLTED JOINT STRENGTH DATA

TEST TEMP. = 350°F

English Units

Sample	e/D	T (in.)	W (in.)	Pin Dia. (in.)	Failure Load (lb_f)	Bearing Stress (10^4PSI)	Shear Stress (10^4PSI)	Net Tension Stress (10^4PSI)	Mode
47L3B	1.85	0.088	0.753	.202	694	3.90	.26	1.43	B
47C3B	1.85	0.092	0.753	.202	673	3.62	.24	1.33	B
47L4B*	1.85	0.091	0.753	.202	496	2.69	.18	0.99	B
47C2B	1.85	0.093	1.002	.202	716	3.81	.26	0.96	B
47C1B	1.85	0.092	0.999	.202	750	4.04	.27	1.02	B
47L2B*	1.85	0.089	1.002	.202	507	2.82	.19	.71	B
47R2T	1.85	0.089	1.504	.202	750	4.17	.28	.65	B
47R1T	1.85	0.091	1.491	.202	783	4.23	.29	.69	B
47L1B*	1.85	0.087	1.496	.202					B

*Indicates test after 4 month storage.

TABLE XII B

$[0/\pm 45/90]_{2s}$ BOLTED JOINT STRENGTH DATA

TEST TEMP. = 177°C (350°F)

S.I. Units

Sample	e/D	T (cm.)	W (cm.)	Pin Dia. (cm.)	Failure Load (Newtons)	Bearing Stress M Pa	Shear Stress M Pa	Net Tension Stress M Pa	Mode
47L3B	1.85	0.224	1.913	0.511	1763	269.0	17.9	98.6	B
47C3B	1.85	0.234	1.913	0.511	1709	249.7	16.6	91.7	B
47C4B	1.85	0.231	1.913	0.511	1260	185.5	12.4	68.3	B
47C2B	1.85	0.236	2.545	0.511	1819	262.8	17.9	66.2	B
47C1B	1.85	0.234	2.537	0.511	1905	278.6	18.6	70.3	B
47L2B	1.85	0.226	2.545	0.511	1288	194.5	13.1	49.0	B
47R2T	1.85	0.226	3.820	0.511	1905	287.6	19.3	44.8	B
47R1T	1.85	0.231	3.787	0.511	1989	291.7	20.0	47.6	B
47L1B	1.85	0.221	3.800	0.511					B

TABLE XIII A

OUT OF PLANE CONSTRAINT BOLTED JOINT STRENGTH DATA

$[0/\pm45/90]_{2s}$ LAMINATE

English Units

Sample	e/D	T (in.)	W (in.)	Pin Dia. (in.)	Failure Load (lb_f)	Bearing Stress (10^4PSI)	Shear Stress (10^4PSI)	Net Tension Stress (10^4PSI)	Mode
46C3B	3.69	0.091	0.754	0.202	1996	10.9	0.31	3.97	B
46R3T	3.69	0.088	0.751	0.202	1974	11.1	0.32	4.09	B
46C2B	3.69	0.090	1.000	0.202	1941	10.7	0.31	2.70	B
45C2B	3.69	0.089	0.996	0.202	2117	11.8	0.34	3.00	B
46C1B	3.69	0.092	1.501	0.202	2294	12.3	0.36	1.92	B
46C1T	3.69	0.090	1.500	0.202	2382	13.1	0.39	2.04	B

TABLE XIII B

OUT OF PLANE CONSTRAINT BOLTED JOINT STRENGTH DATA

$[0/\pm45/90]_{2s}$ LAMINATE

S.I. Units

Sample	e/D	T (cm.)	W (cm.)	Pin Dia. (cm.)	Failure Load (Newtons)	Bearing Stress M Pa	Shear Stress M Pa	Net Tension Stress M Pa	Mode
46C3B	3.69	0.231	1.915	0.513	8882	751.6	21.4	273.7	B
46R3T	3.69	0.224	1.908	0.513	8784	765.3	22.1	282.0	B
46C2B	3.69	0.229	2.540	0.513	8637	737.8	21.4	186.2	B
45C2B	3.69	0.226	2.530	0.513	9420	813.6	23.4	206.9	B
46C1B	3.69	0.234	3.813	0.513	10208	848.1	24.8	132.4	B
46C1T	3.69	0.229	3.810	0.513	10600	903.2	26.9	140.7	B

TABLE XIV A

OUT OF PLANE CONSTRAINT BOLTED JOINT STRENGTH DATA

$[0/\pm45/90]_{2s}$ LAMINATE

English Units

Sample	e/D	T (in.)	W (in.)	Pin Dia. (in.)	Failure Load (lb_f)	Bearing Stress (10^4PSI)	Shear Stress (10^4PSI)	Net Tension Stress (10^4PSI)	Mode
46R3B	1.85	0.089	0.752	0.202	1875	10.4	0.70	3.84	B
45R4T	1.85	0.089	0.749	0.202	1919	10.7	0.72	3.94	B
47R3T	1.85	0.091	1.005	0.202	2007	10.9	0.74	2.75	B
46L2B	1.85	0.090	1.500	0.202	1941	10.7	0.72	1.66	B
45C1B	1.85	0.088	1.495	0.202	2051	11.5	0.78	1.80	B

TABLE XIV B

OUT OF PLANE CONSTRAINT BOLTED JOINT DATA

$[0/\pm 45/90]_{2s}$ LAMINATE

S.I. Units

Sample	e/D	T (cm.)	W (cm.)	Pin Dia. (cm.)	Failure Load (Newtons)	Bearing Stress M Pa	Shear Stress M Pa	Net Tension Stress M Pa	Mode
46R3B	1.85	0.226	1.910	0.513	8344	717.1	48.3	264.8	B
45R4T	1.85	0.226	1.902	0.513	8539	737.8	49.6	271.7	B
47R3T	1.85	0.231	2.553	0.513	8931	751.6	51.0	189.6	B
46L2B	1.85	0.229	3.810	0.513	8637	737.8	49.6	114.5	B
45C1B	1.85	0.224	3.797	0.513	9126	792.9	53.8	124.1	B

TABLE XV A

OUT OF PLANE CONSTRAINT BOLTED JOINT STRENGTH DATA

$[45/0/-45/0_2/-45/0/45/0_2/90]_s$ LAMINATE

English Units

Sample	e/D	T (in.)	W (in.)	Pin Dia. (in.)	Load	Bearing Stress (10^4PSI)	Shear Stress (10^4PSI)	Net Tension Stress (10^4PSI)	Mode
04L4B	1.85	0.122	0.753	0.202	2427	9.85	0.66	3.61	S/NT
04L5B	1.85	0.125	0.754	0.202	2482	9.83	0.66	3.60	S/NT
04R4T	1.85	0.126	1.004	0.202	2427	9.54	0.64	2.40	S
04R4B	1.85	0.125	1.003	0.202	2294	9.09	0.61	2.29	S
04C1T	1.85	0.124	1.498	0.202	2250	8.98	0.61	1.40	S
04L1B	1.85	0.124	1.498	0.202	2206	8.81	0.59	1.37	S

TABLE XV B

OUT OF PLANE CONSTRAINT BOLTED JOINT STRENGTH DATA

$[45/0/-45/0_2/-45/0/45/0_2/90]_s$ LAMINATE

S.I. Units

Sample	e/D	T (cm.)	W (cm.)	Pin Dia. (cm.)	Failure Load (Newtons)	Bearing Stress M Pa	Shear Stress M Pa	Net Tension Stress M Pa	Mode
04L4B	1.85	0.310	1.913	0.513	10,800	679.2	45.5	248.9	S/NT
04L5B	1.85	0.318	1.915	0.513	11,045	677.8	45.5	248.2	S/NT
04R4T	1.85	0.320	2.550	0.513	10,800	657.8	44.1	165.5	S
04R4B	1.85	0.318	2.548	0.513	10,208	626.8	42.1	157.9	S
04C1T	1.85	0.315	3.805	0.518	10,012	619.2	42.1	96.5	S
04L1B	1.85	0.315	3.805	0.513	9,816	607.4	40.7	95.4	S

TABLE XVI COMPARISON OF EXPERIMENTAL AND FINITE ELEMENT MODEL NET SECTION STRAIN CONCENTRATIONS

Case	W in./cm	e/D	E_x Finite Element PSIx10^6/ GPa	E_x Experi. PSIx10^6/ GPa	K_{nt_f} Finite Element	K_{nt_e} Experi.
1	.75/1.91	4	11.4/ 78.6	11.23/ 77.7	3.01	3.06
2	.75/1.91	4	7.13/ 49.2	6.82/ 47.0	3.26	3.10
3	.75/1.91	2	11.4/ 78.6	9.62/ 66.3	2.11	2.13
4	.75/1.91	2	7.13/ 49.2	6.83/ 47.2	2.43	2.57

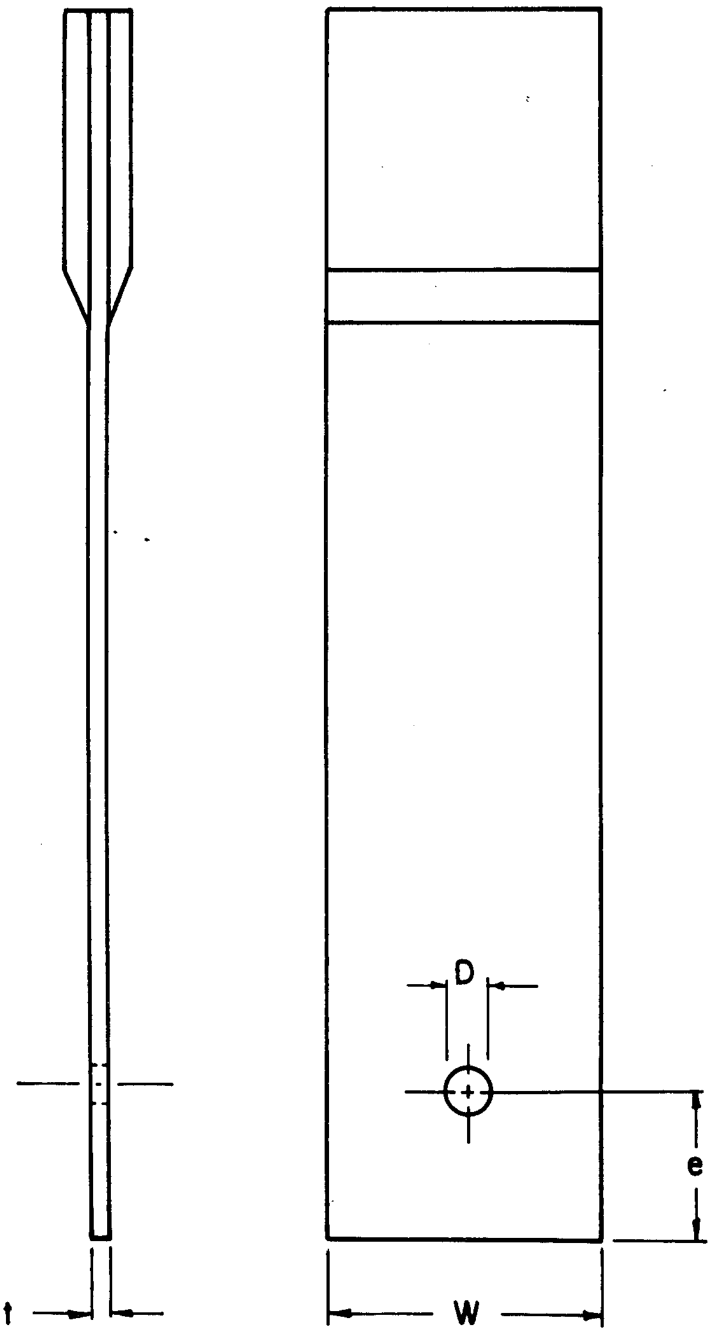

FIGURE 2.2.1 - BOLTED JOINT TEST COUPON GEOMETRY

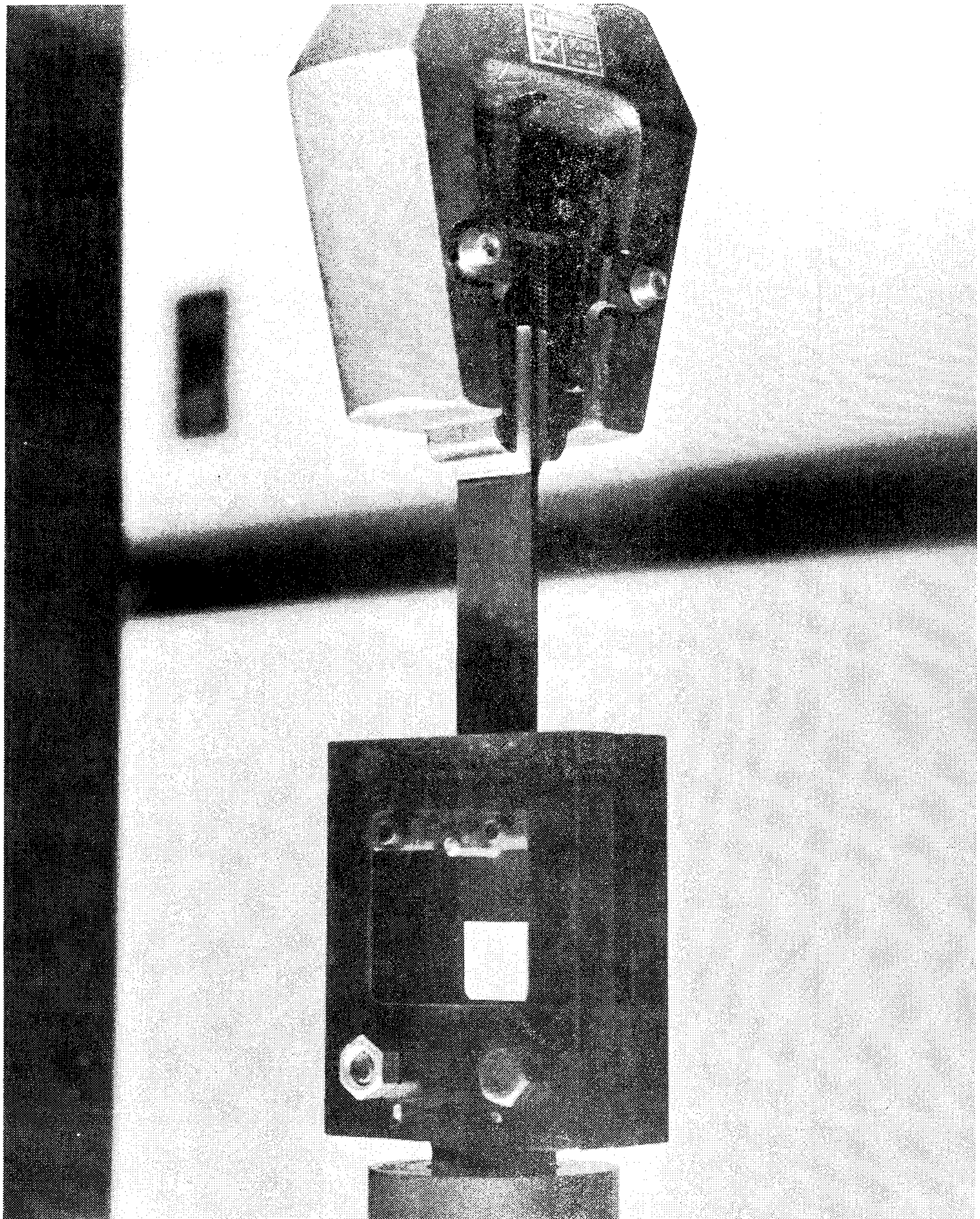

FIGURE 2.3.1 - BOLTED JOINT TEST FIXTURE USED FOR PIN-BEARING TESTS

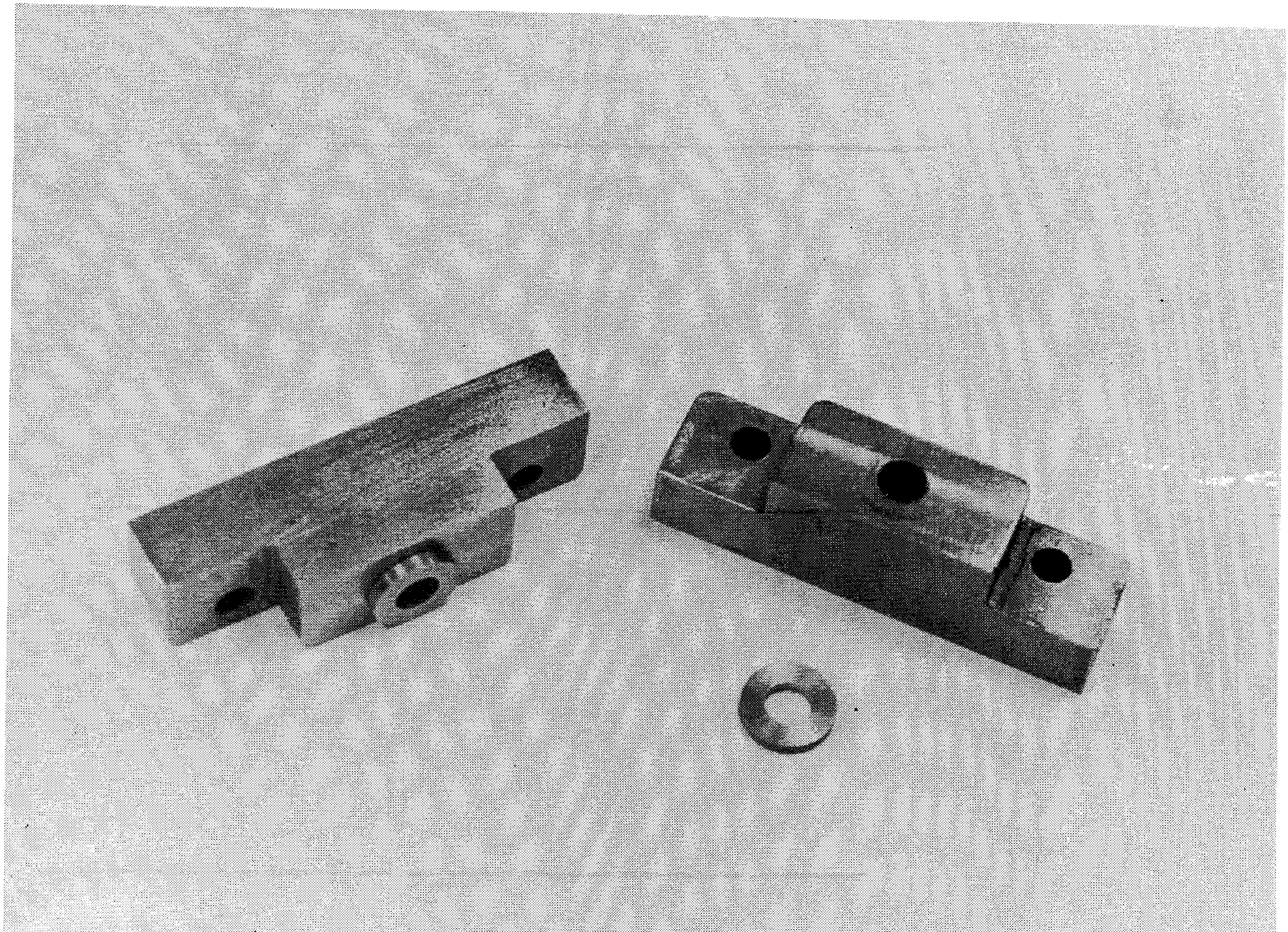

FIGURE 2.3.2 - INSERTS USED TO APPLY OUT-OF-PLANE CONSTRAINTS

Strain Gage Locations

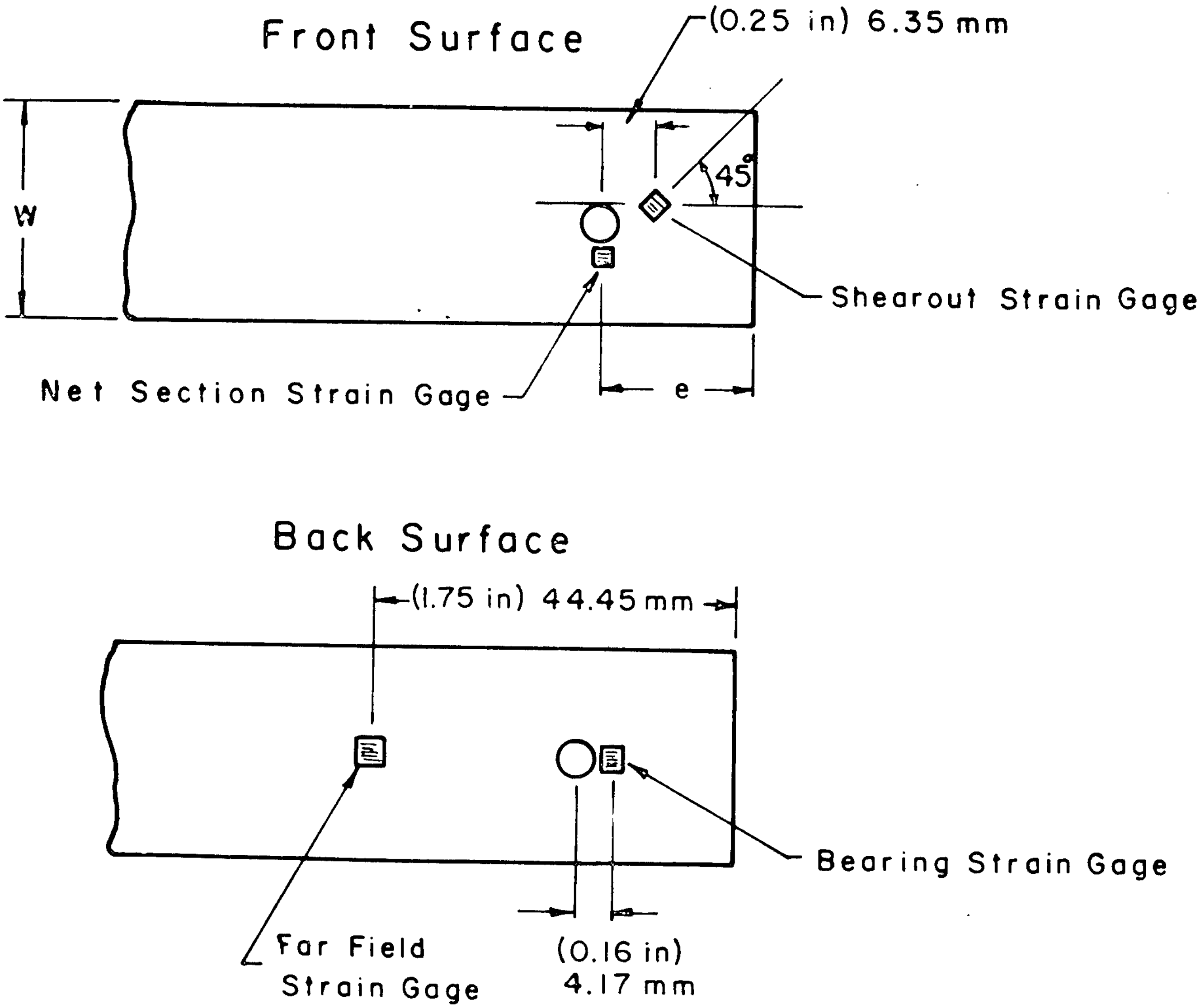

FIGURE 2.4.1 - INSTRUMENTATION LOCATIONS ON TEST COUPON

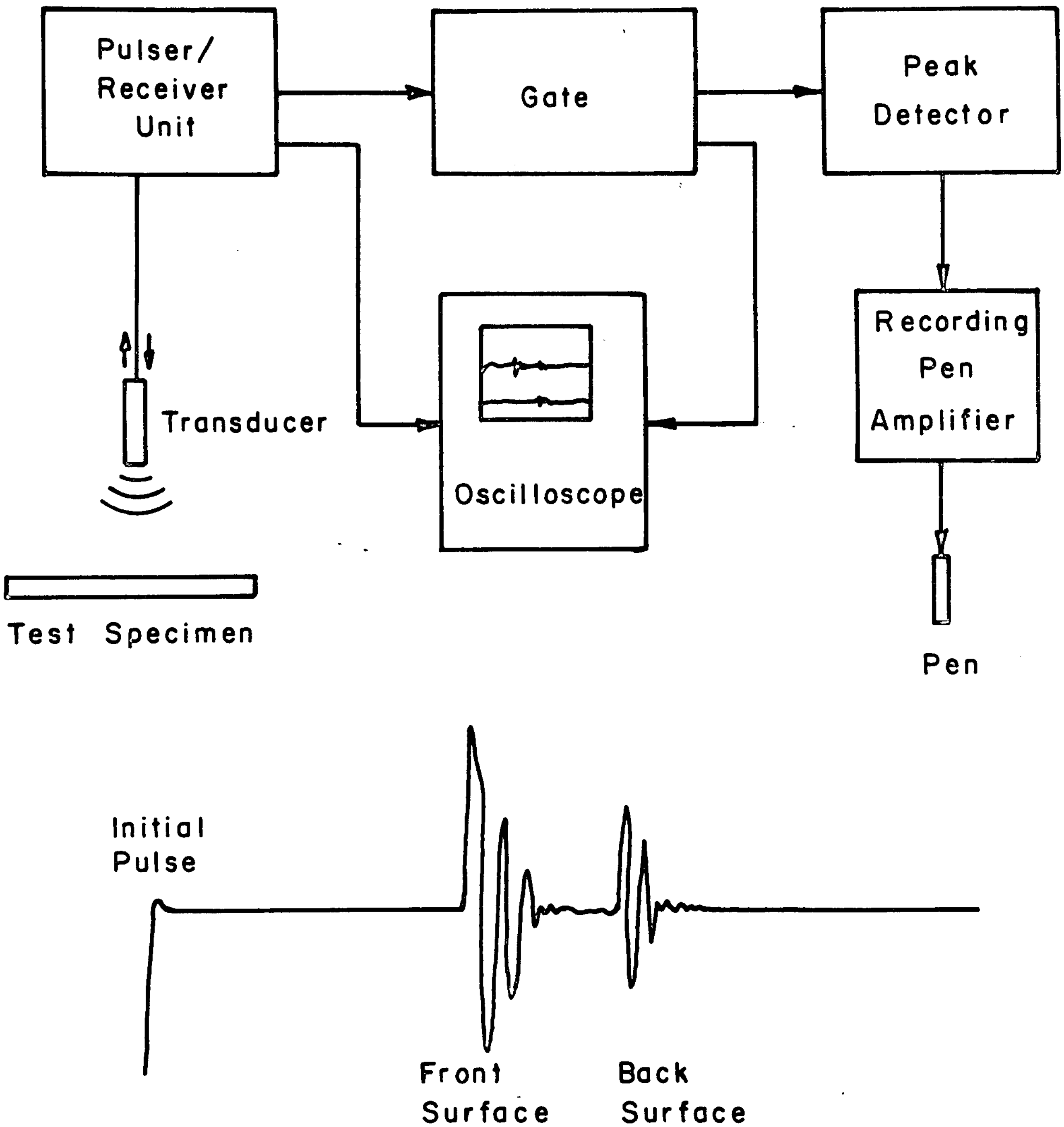

FIGURE 2.6.1 - ULTRASONIC "C" SCAN BLOCK DIAGRAM

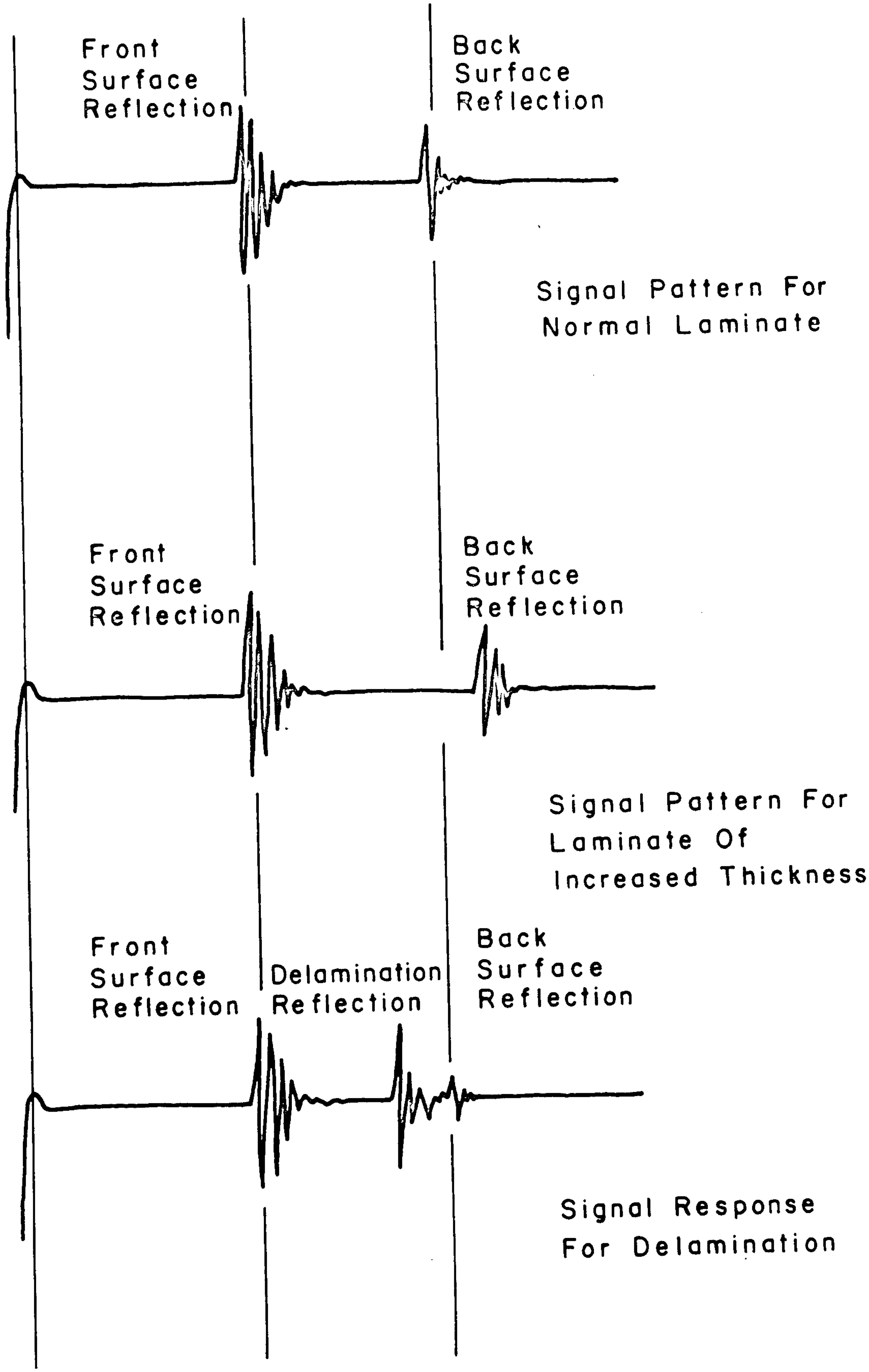

FIGURE 2.6.2 - SIGNAL WAVEFORMS CHARACTERISTIC OF DEFECTS

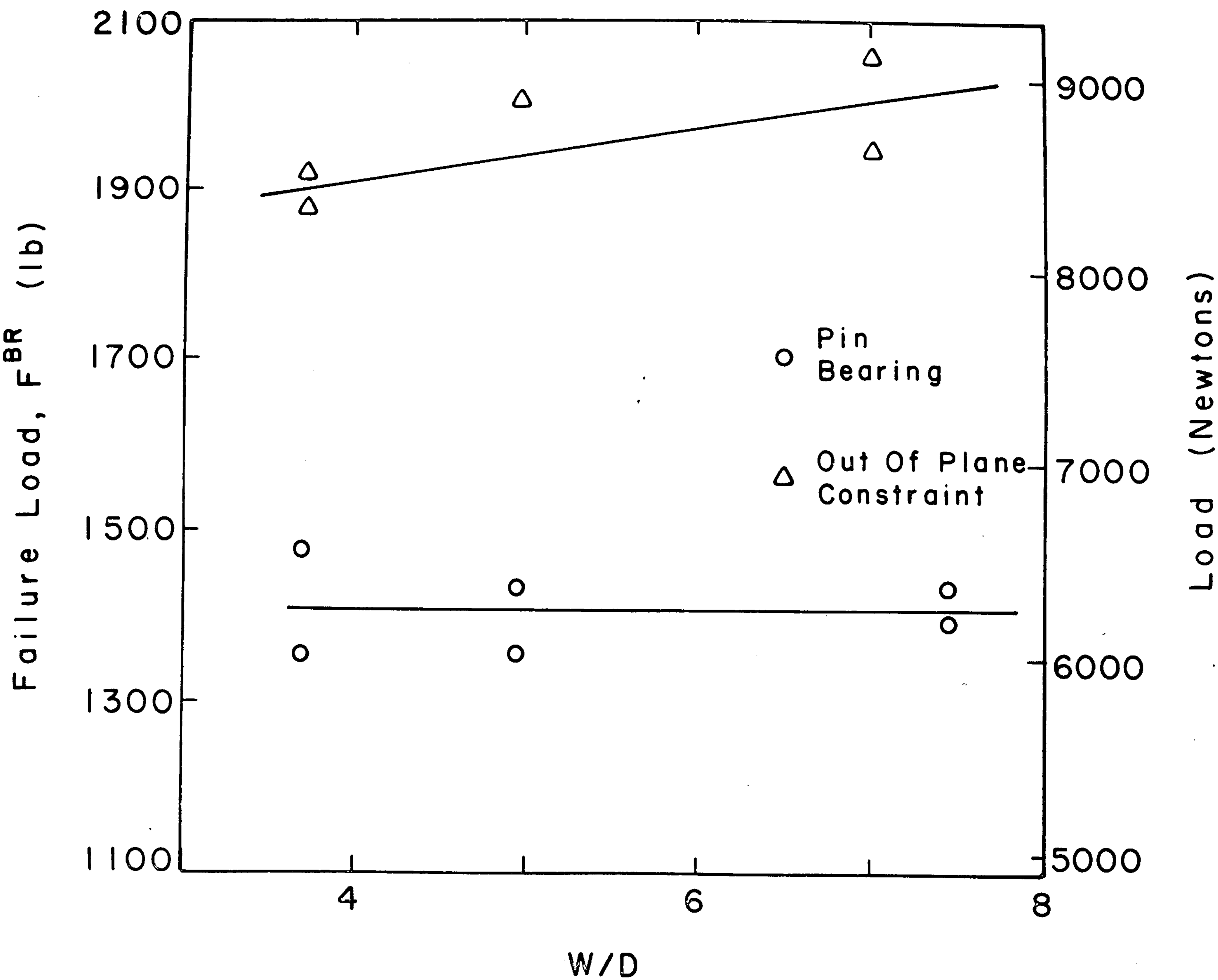

FIGURE 3.1.1 - COMPARISON OF PIN LOADED AND OUT-OF-PLANE CONSTRAINT STRENGTH FOR AS/3501-6 GRAPHITE EPOXY QUASI-ISOTROPIC LAMINATE, e/D = 1.85

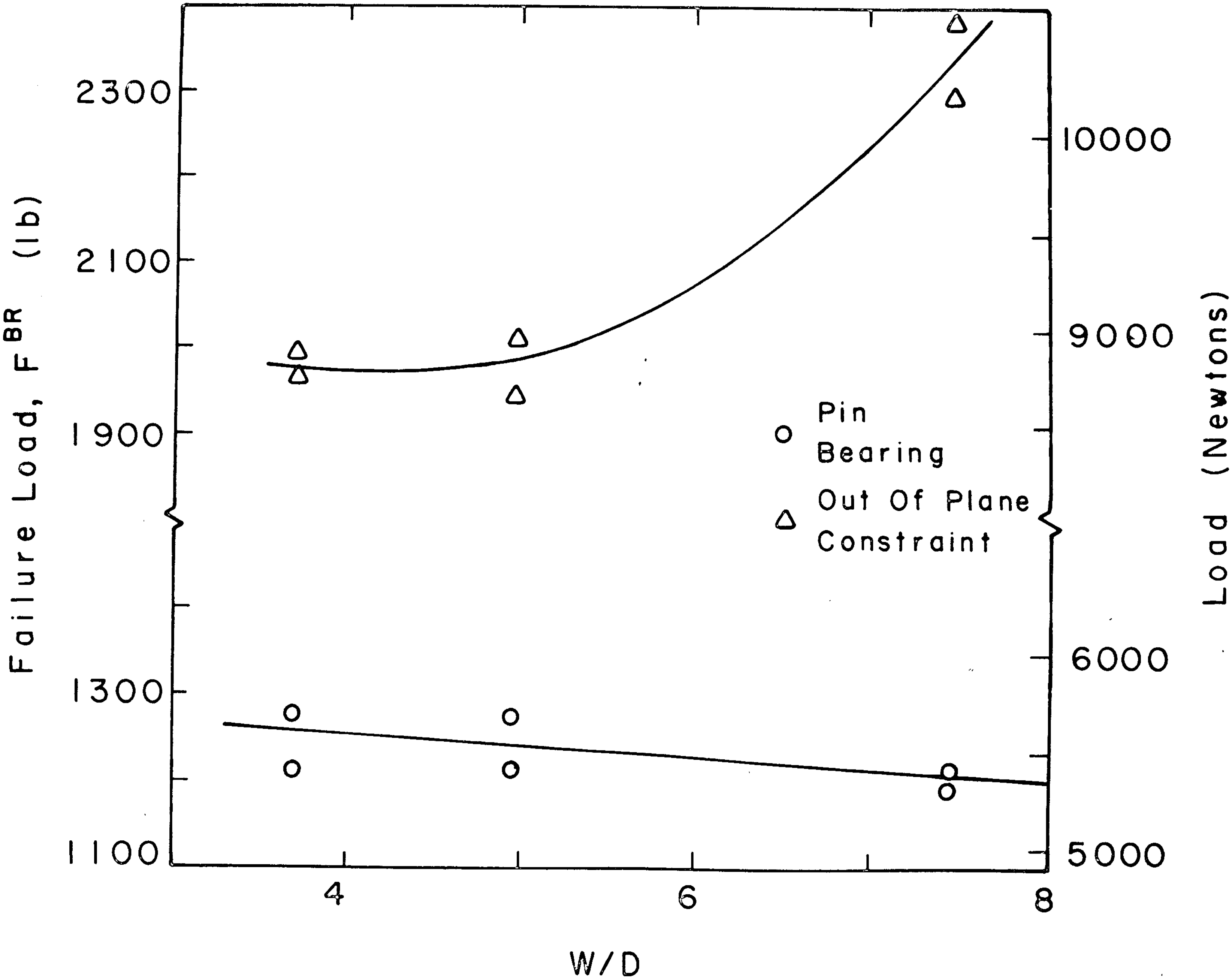

FIGURE 3.1.2 - COMPARISON OF PIN LOADED AND OUT-OF-PLANE CONSTRAINT STRENGTH FOR AS/3501-6 GRAPHITE EPOXY QUASI-ISOTROPIC LAMINATE, e/D = 3.69

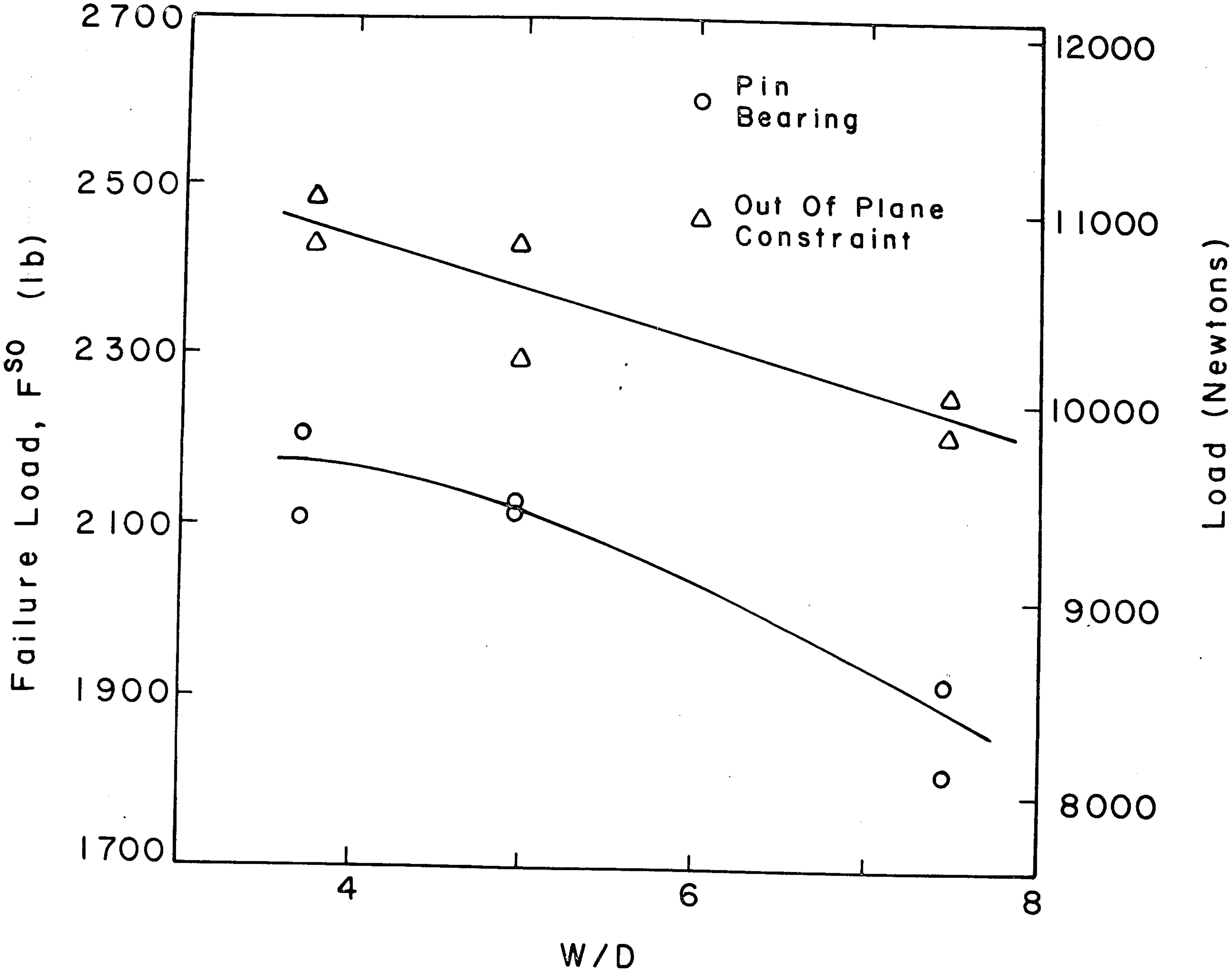

FIGURE 3.1.3 - COMPARISON OF PIN LOADED AND OUT-OF-PLANE CONSTRAINT STRENGTH FOR AS/3501-6 GRAPHITE EPOXY 0° DOMINATED LAMINATE

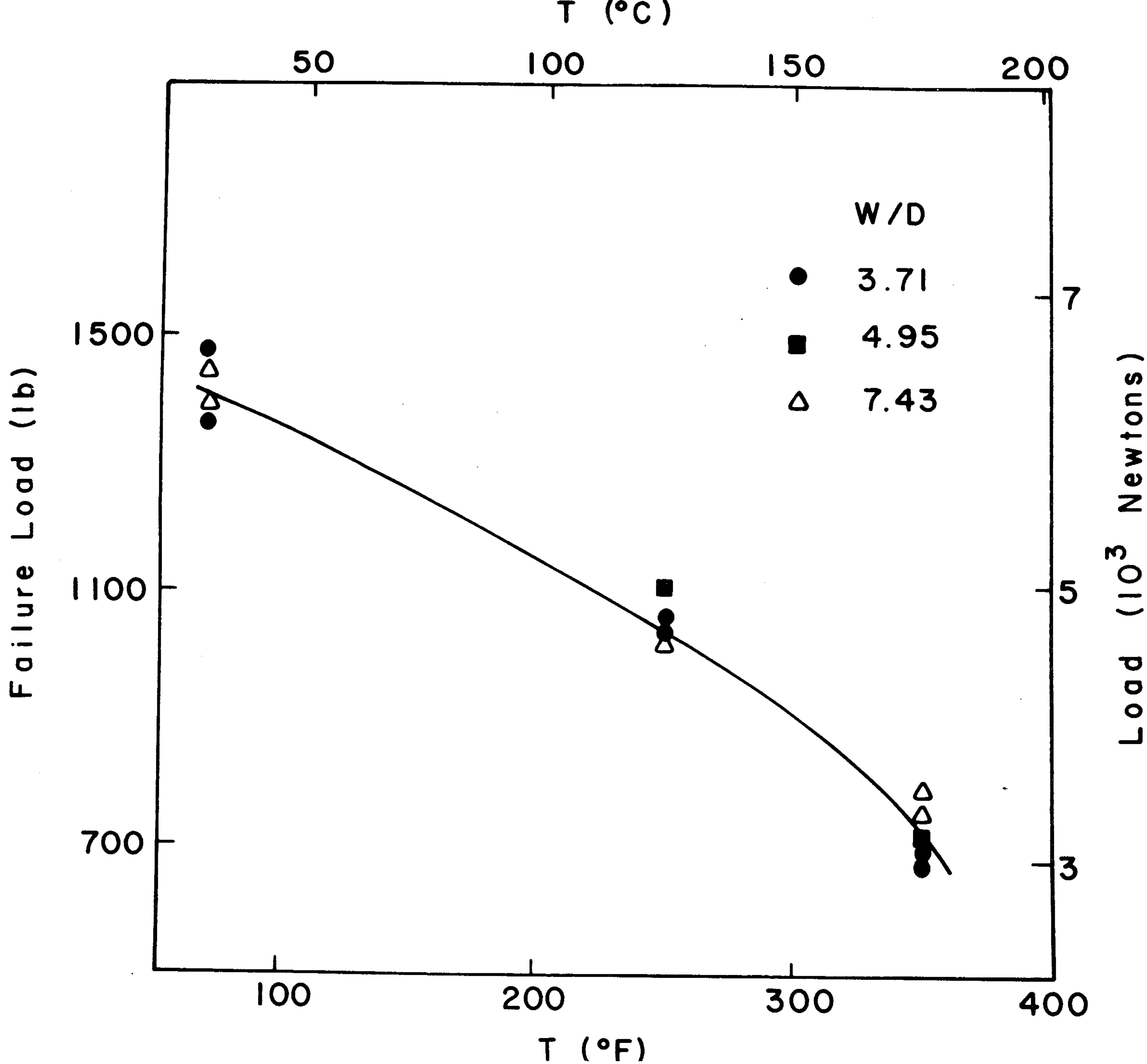

FIGURE 3.2.1 - FAILURE LOAD VERSUS TEMPERATURE FOR AS/3501-6 GRAPHITE EPOXY QUASI-ISOTROPIC LAMINATE, e/D = 1.85

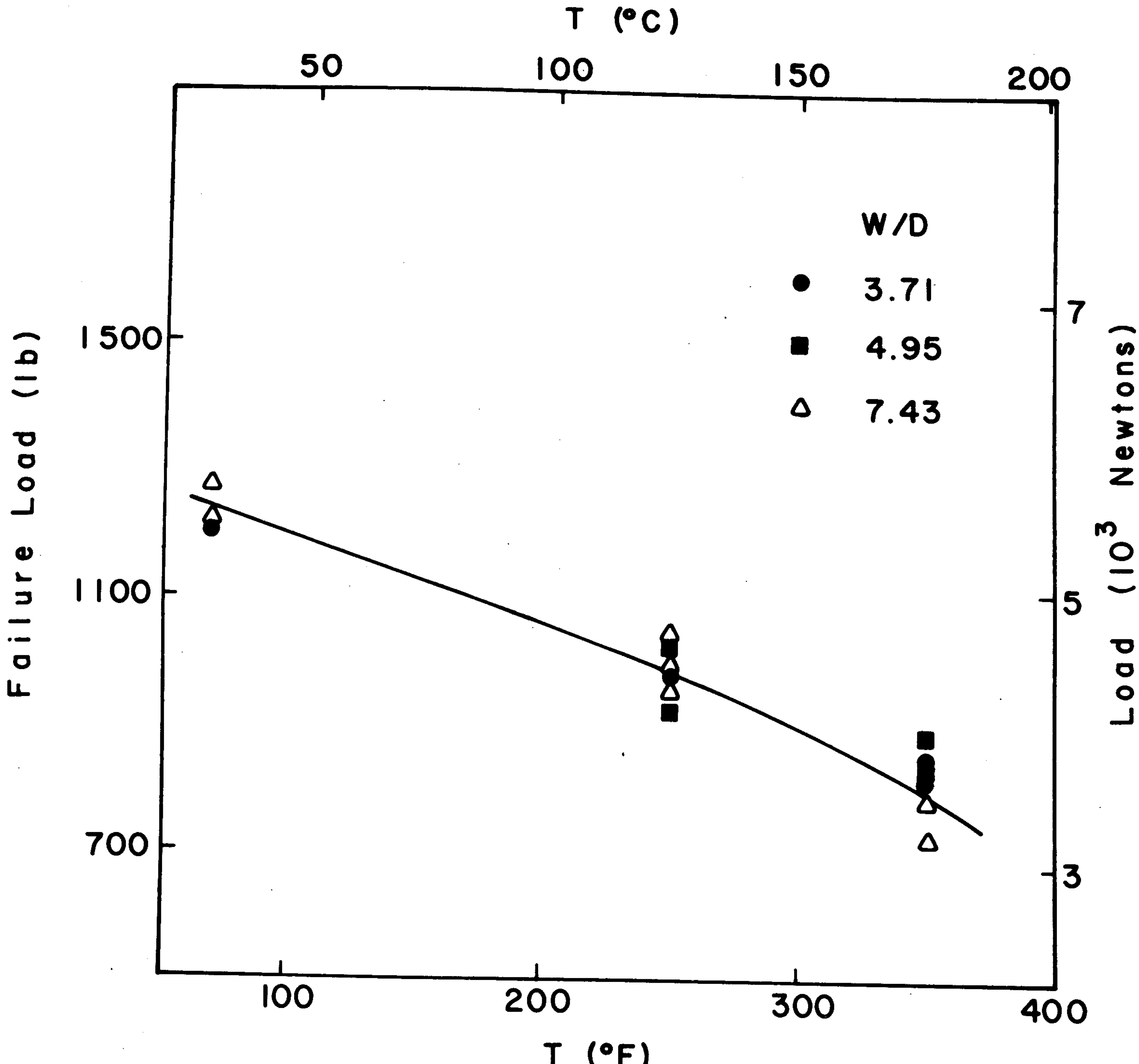

FIGURE 3.2.2 - FAILURE LOAD VERSUS TEMPERATURE FOR AS/3501-6 GRAPHITE EPOXY QUASI-ISOTROPIC LAMINATE, [illegible]/D = 3.69

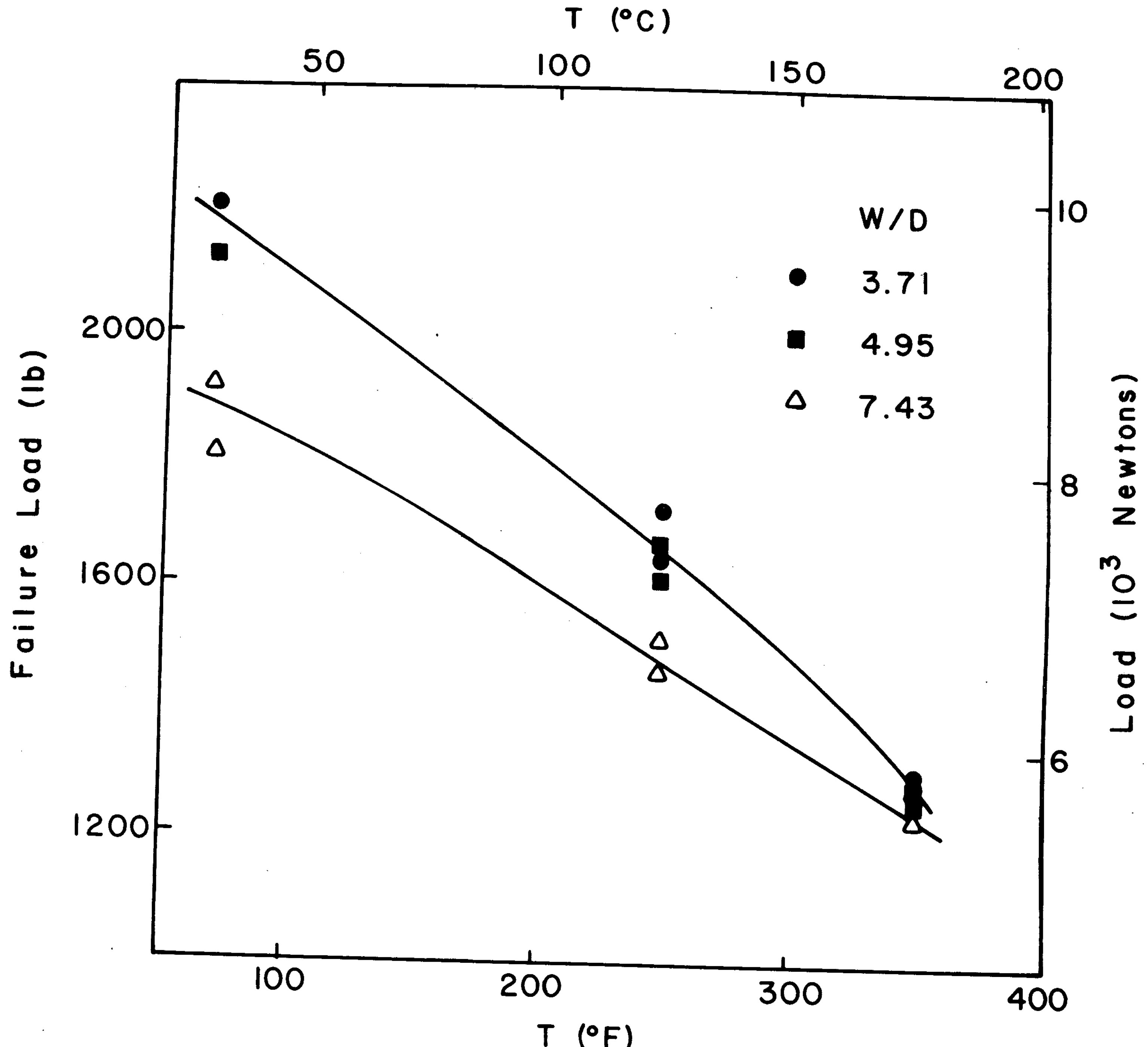

FIGURE 3.2.3 - FAILURE LOAD VERSUS TEMPERATURE FOR AS/3501-6 GRAPHITE EPOXY
0^{o} DOMINATED LAMINATE, e/D = 1.85

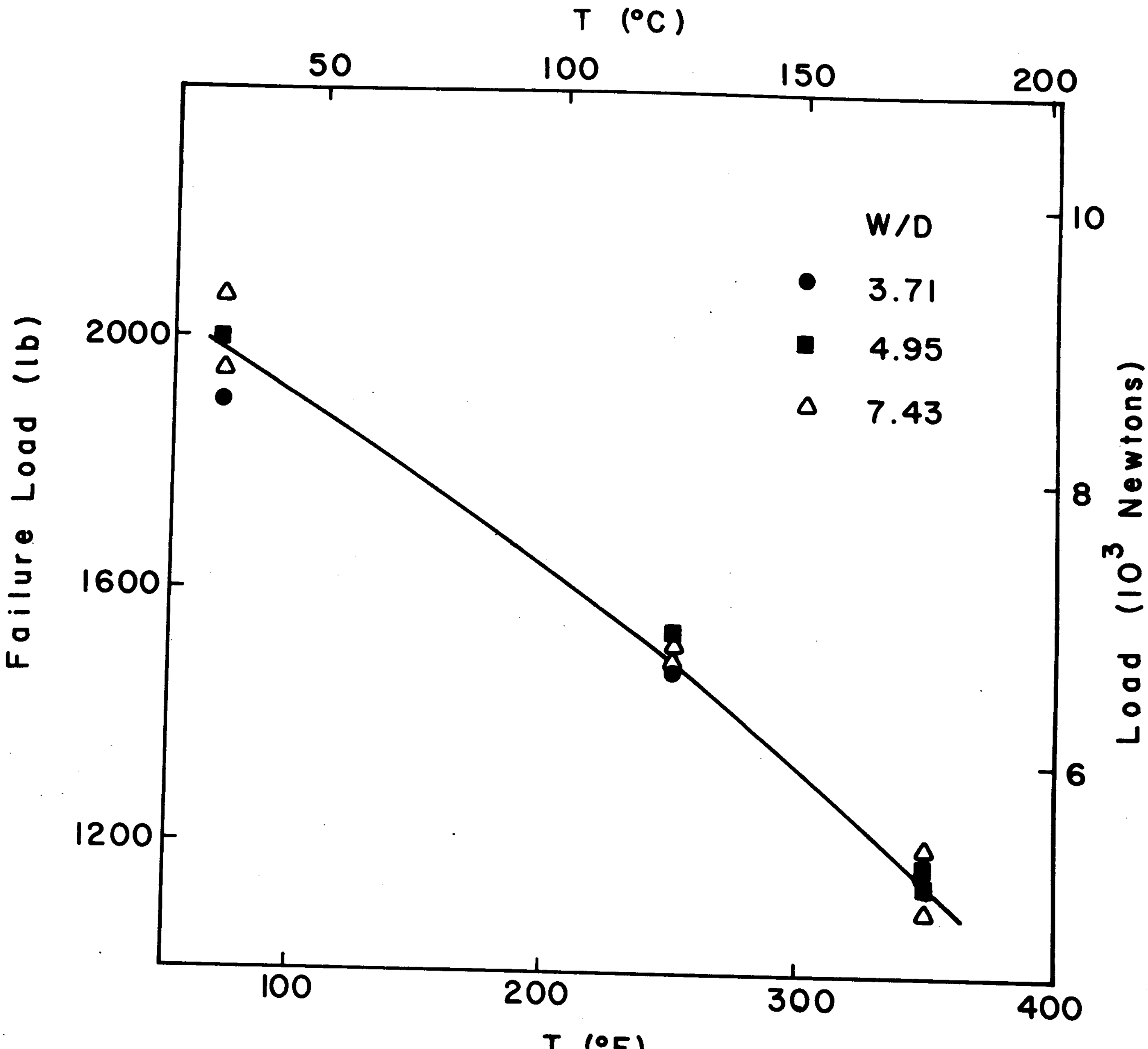

FIGURE 3.2.4 - FAILURE LOAD VERSUS TEMPERATURE FOR AS/3501-6 GRAPHITE EPOXY 0^o DOMINATED LAMINATE, e/D = 3.69

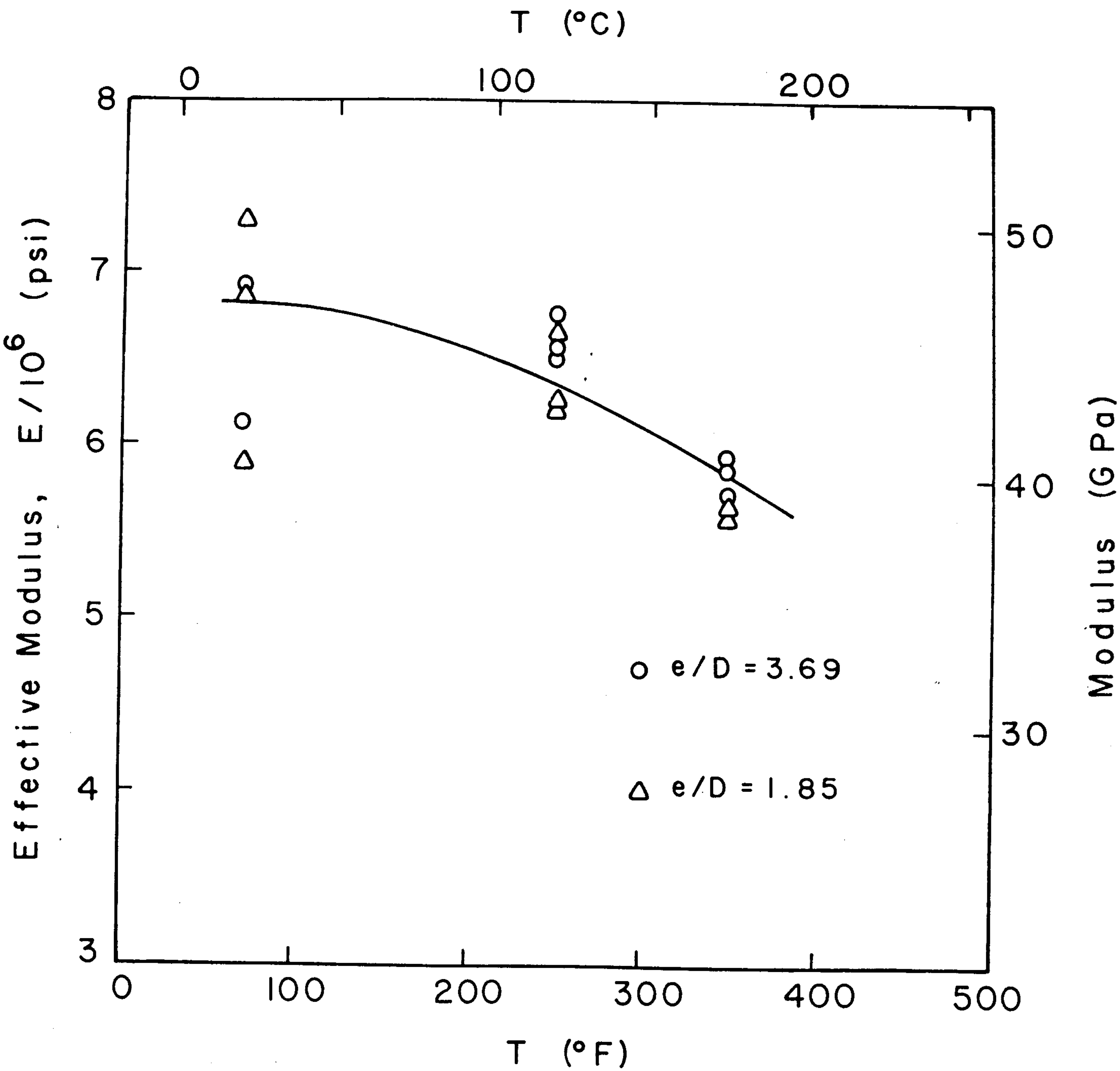

FIGURE 3.3.1 - VARIATION OF LAMINATE MODULUS WITH TEMPERATURE FOR QUASI-ISOTROPIC LAMINATE

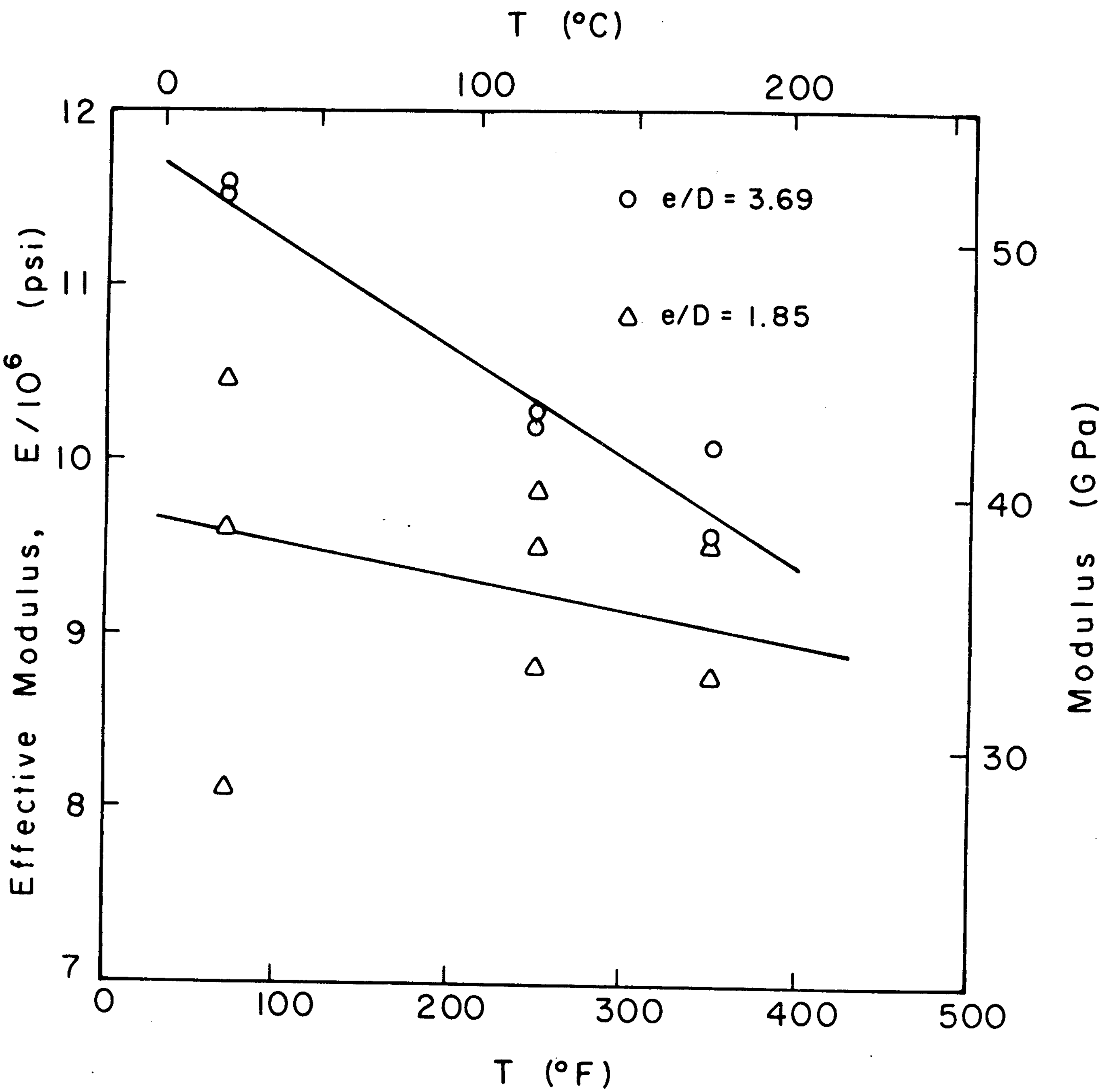

FIGURE 3.3.2 - VARIATION OF LAMINATE MODULUS WITH TEMPERATURE FOR 0^0 DOMINATED LAMINATE

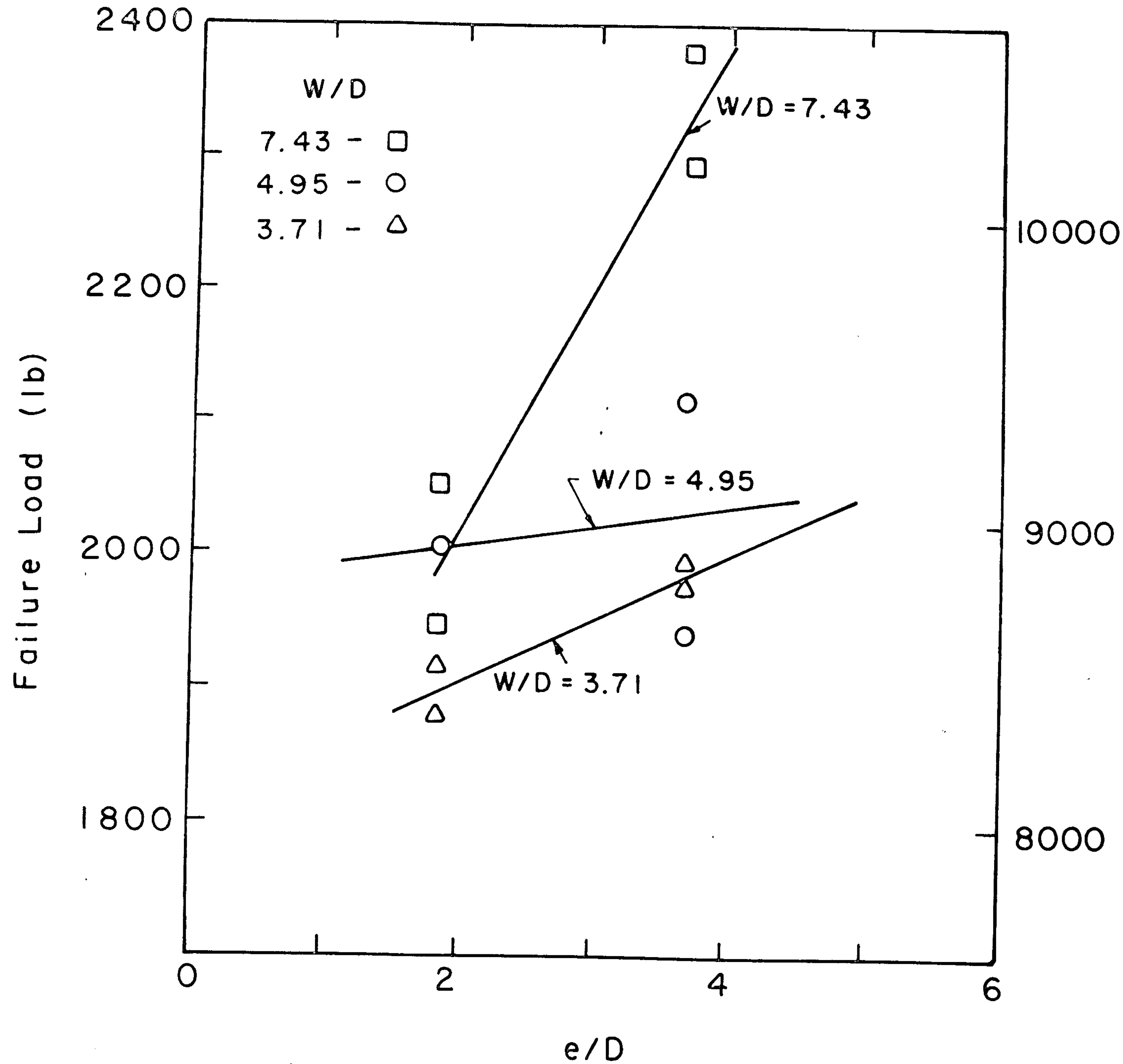

FIGURE 3.4.1 - FAILURE LOAD VERSUS e/D FOR AS/3501-6 GRAPHITE EPOXY QUASI-ISOTROPIC LAMINATE WITH OUT-OF-PLANE CONSTRAINTS

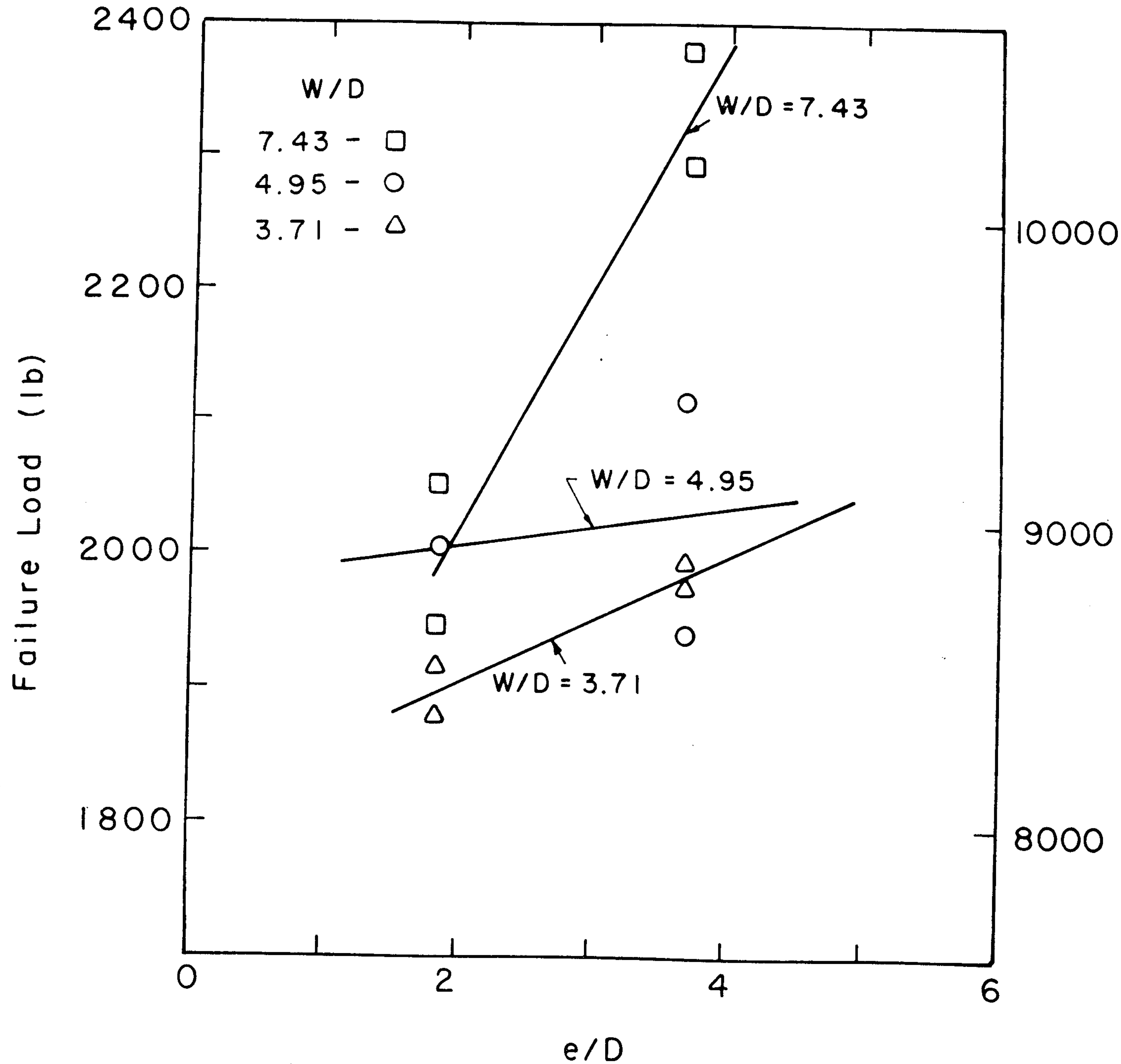

FIGURE 3.4.1 - FAILURE LOAD VERSUS e/D FOR AS/3501-6 GRAPHITE EPOXY QUASI-ISOTROPIC LAMINATE WITH OUT-OF-PLANE CONSTRAINTS

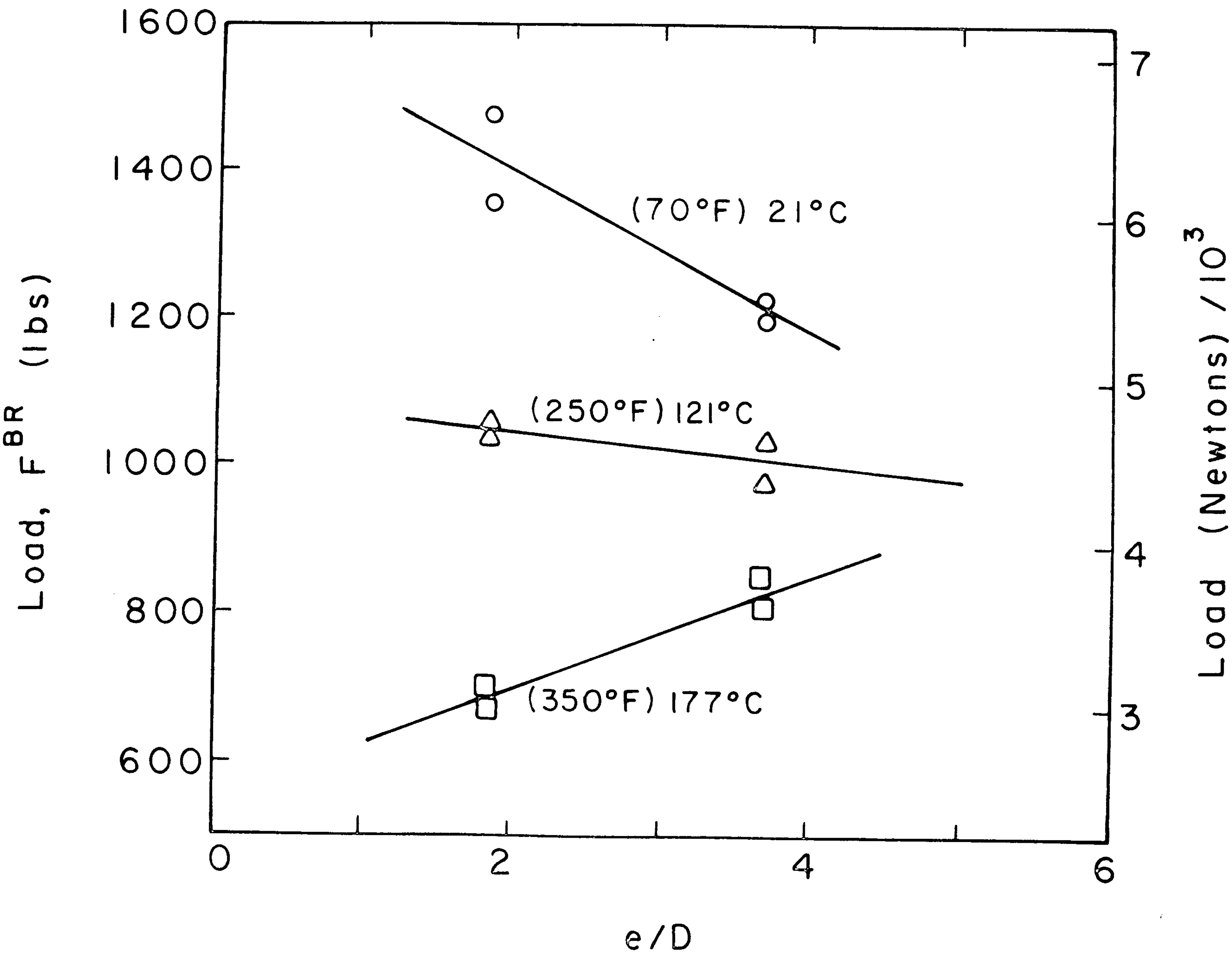

FIGURE 3.4.2 - PIN BEARING FAILURE LOAD VERSUS e/D FOR QUASI-ISOTROPIC LAMINATE, W/D = 3.71

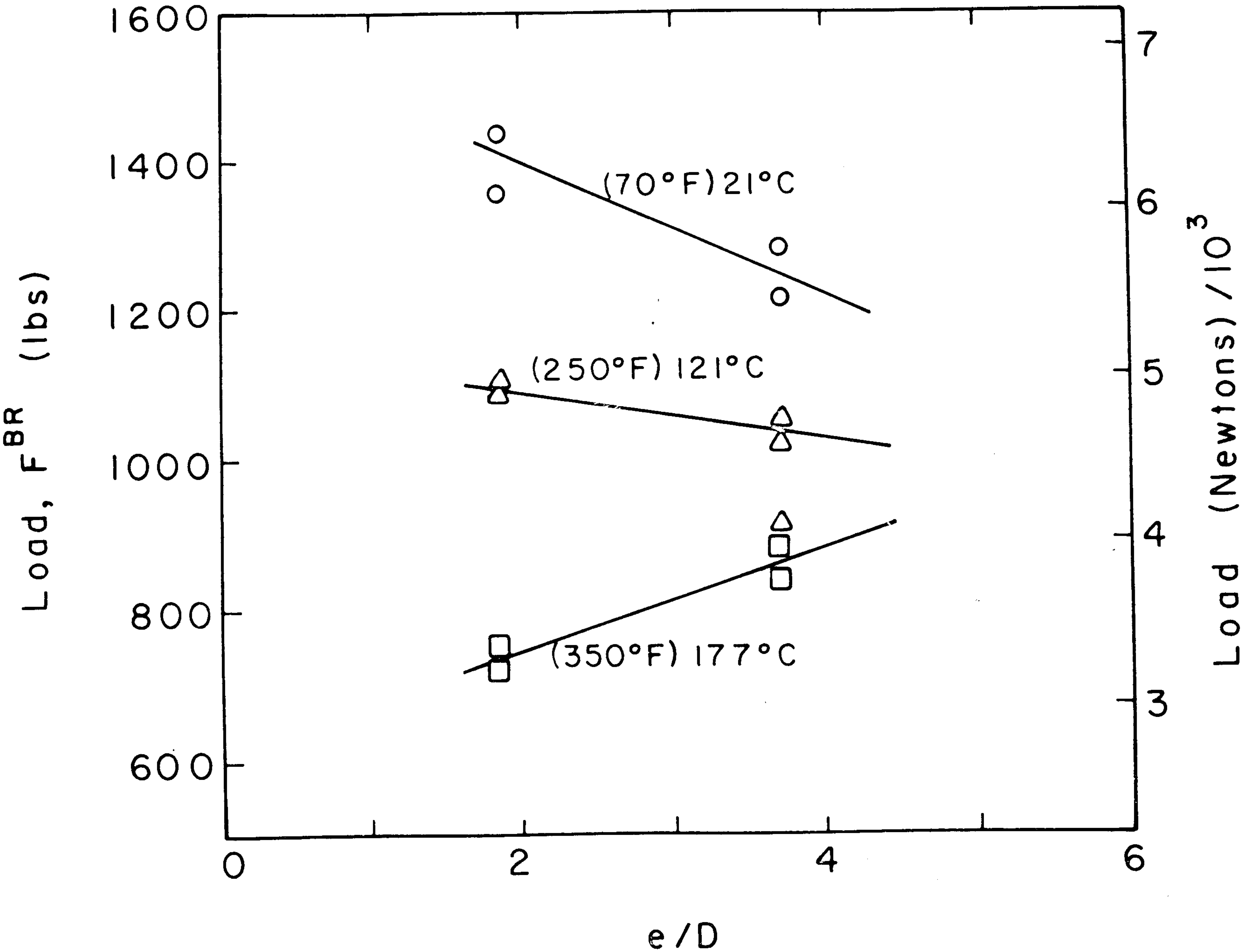

FIGURE 3.4.3 - PIN BEARING FAILURE LOAD VERSUS e/D FOR QUASI-ISOTROPIC LAMINATE, W/D = 4.95

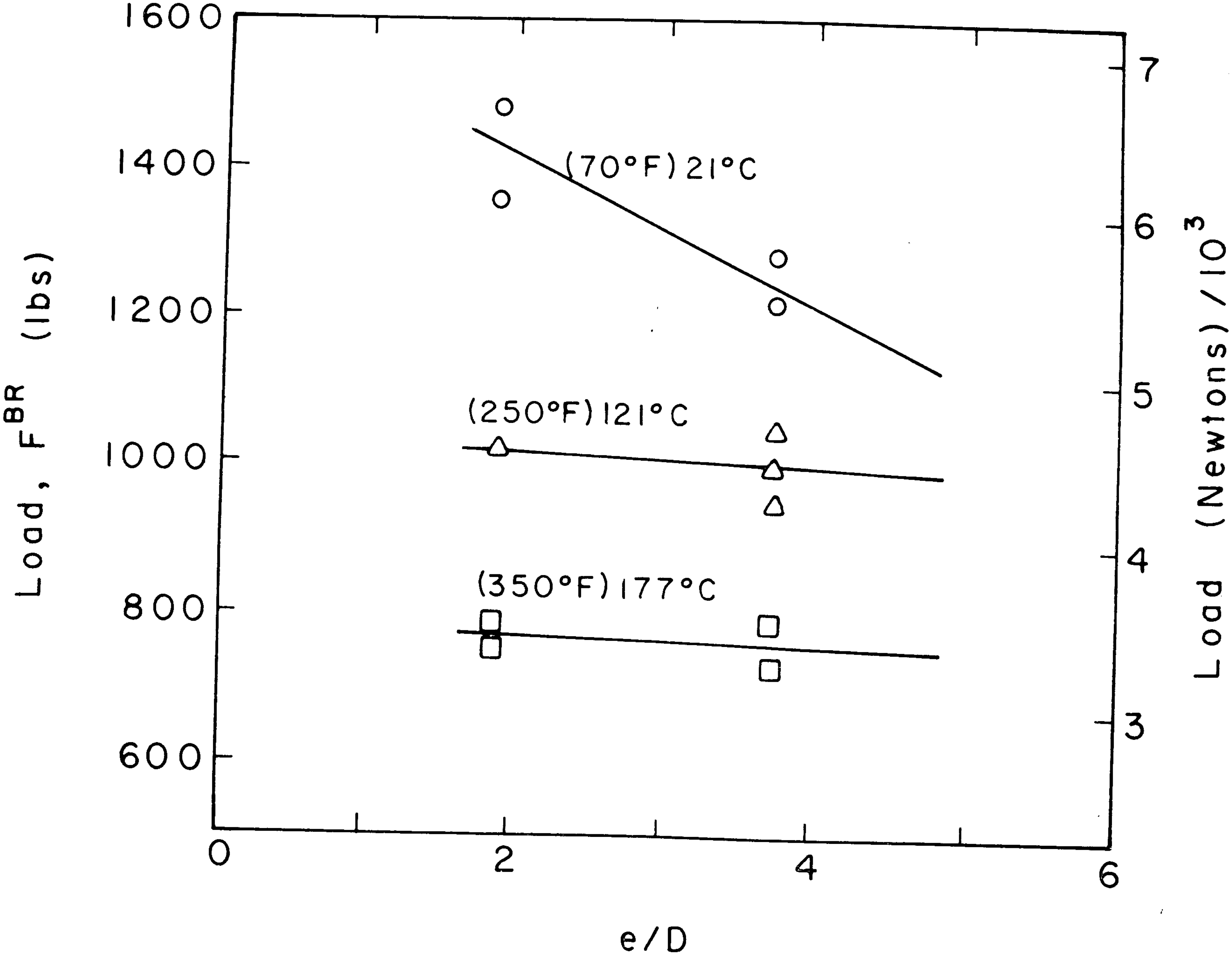

FIGURE 3.4.4 - PIN BEARING FAILURE LOAD VERSUS e/D FOR QUASI-ISOTROPIC LAMINATE, W/D = 7.43

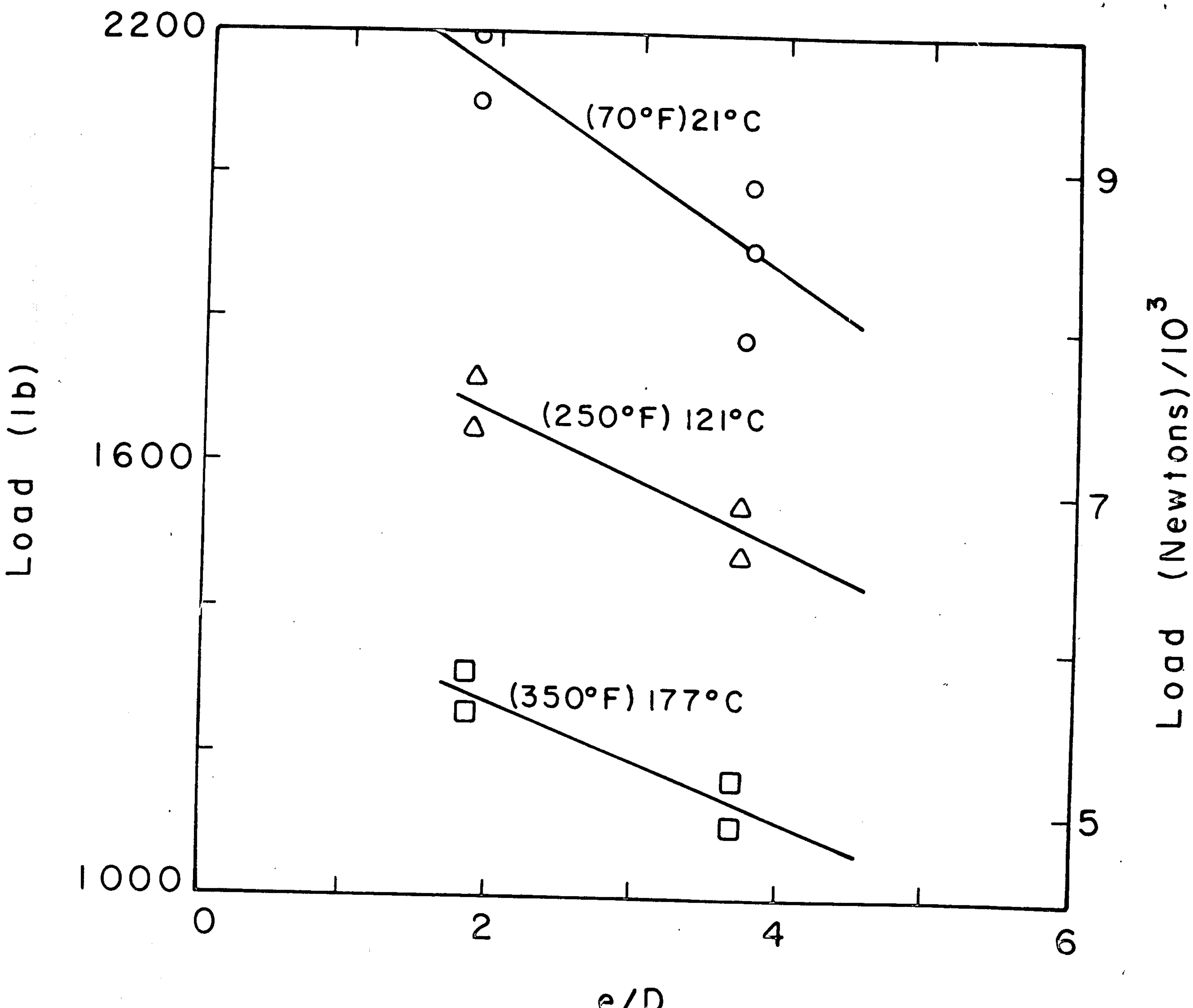

FIGURE 3.5.1 - PIN BEARING FAILURE LOAD VERSUS e/D FOR 0° DOMINATED LAMINATE, W/D = 3.71

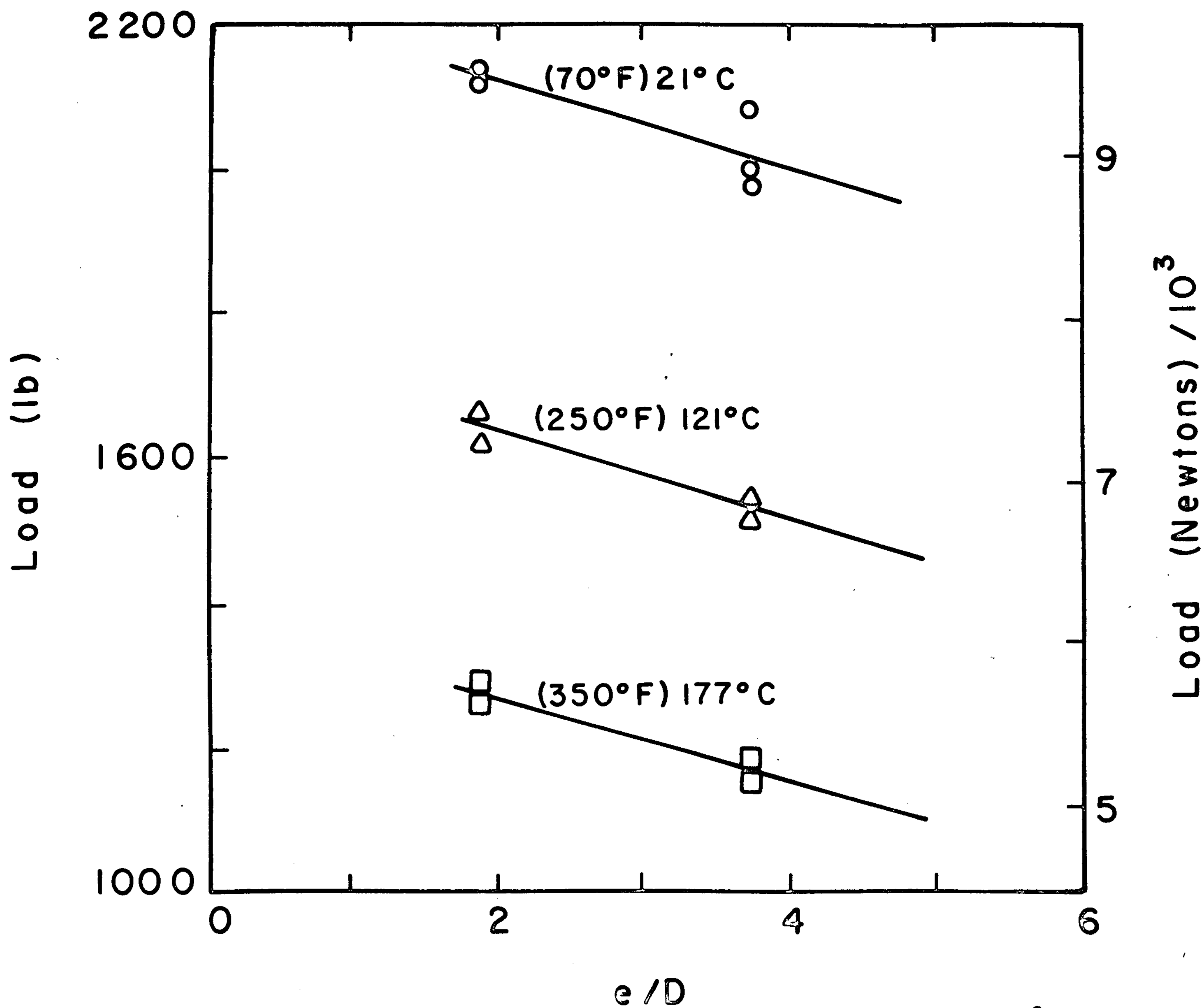

FIGURE 3.5.2 - PIN BEARING FAILURE LOAD VERSUS e/D FOR 0° DOMINATED LAMINATE, W/D = 4.95

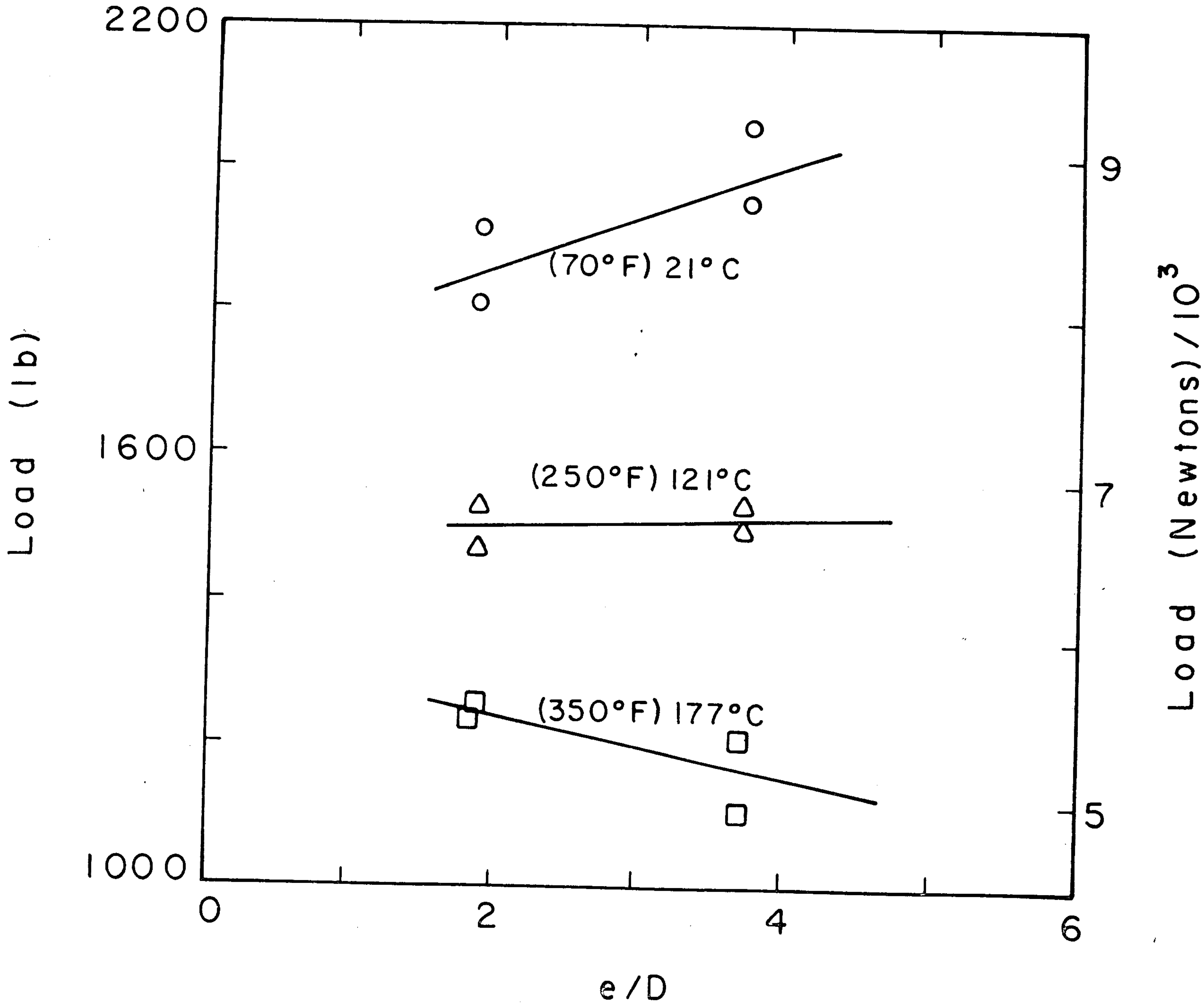

FIGURE 3.5.3 - PIN BEARING FAILURE LOAD VERSUS e/D FOR 0° DOMINATED LAMINATE, W/D = 7.43

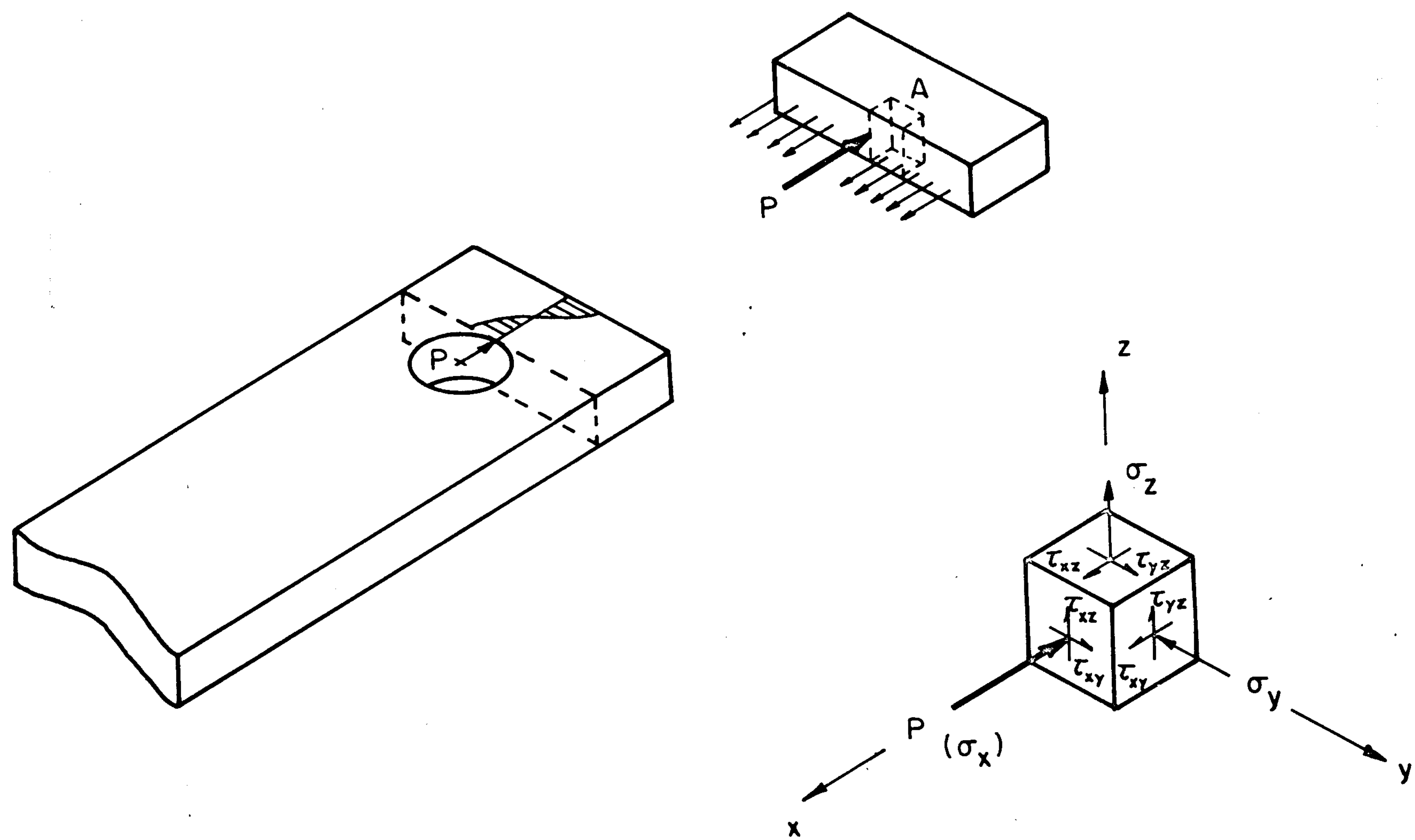

FIGURE 3.5.4 - BEAM BENDING ANALOGY FOR PIN LOADED JOINT

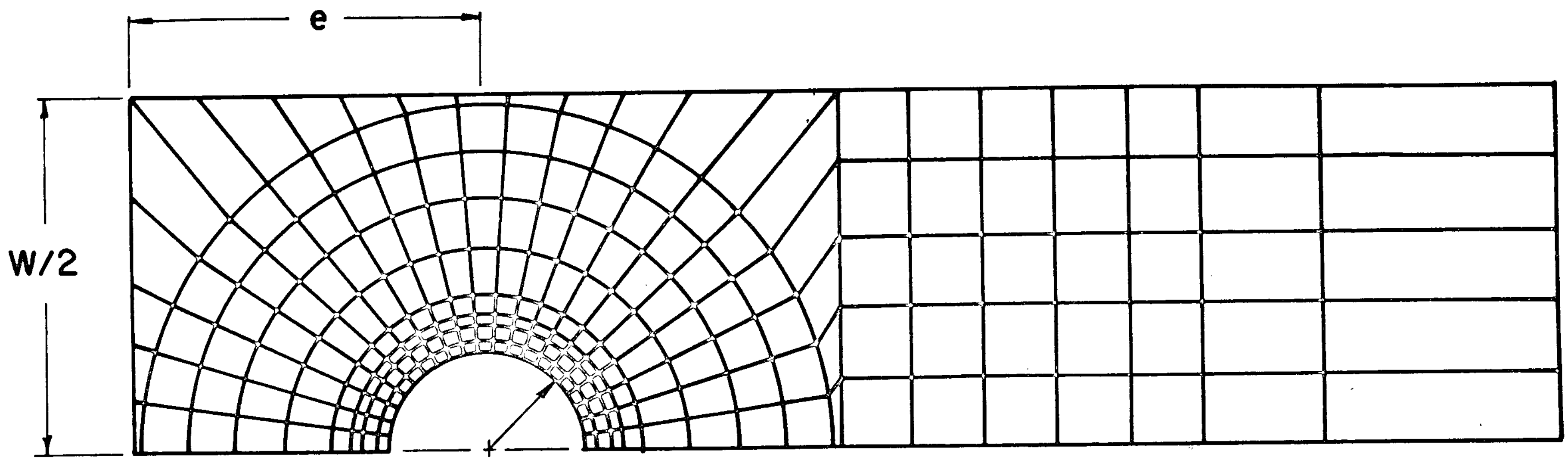

FIGURE 3.6.1 - FINITE ELEMENT MODEL OF e/D = 2 PIN LOADED JOINT

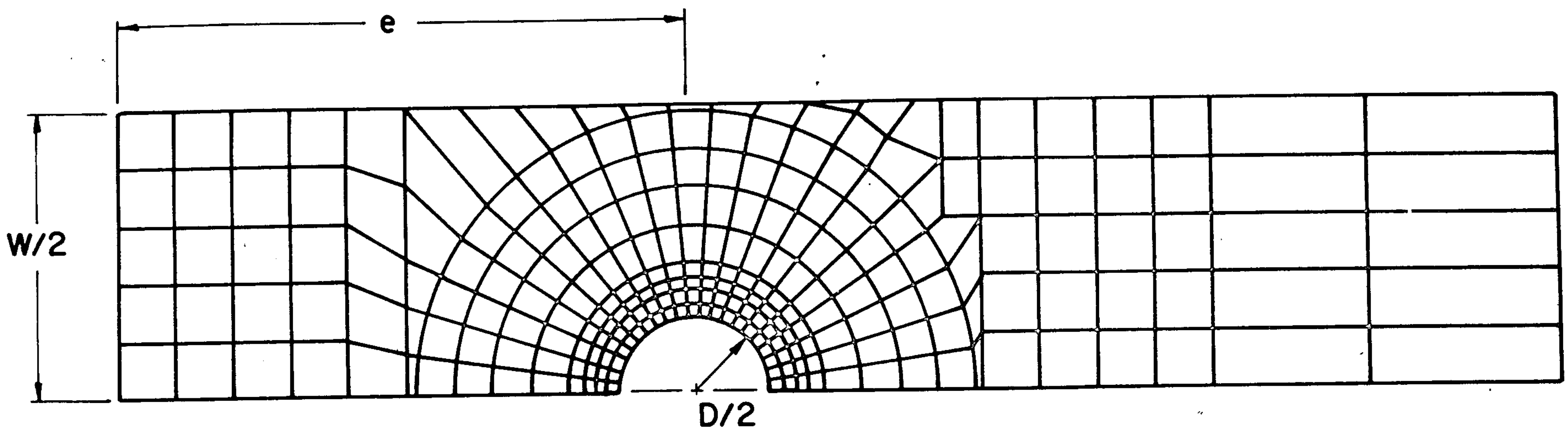

FIGURE 3.6.2 - FINITE ELEMENT MODEL OF e/D = 4 PIN LOADED JOINT

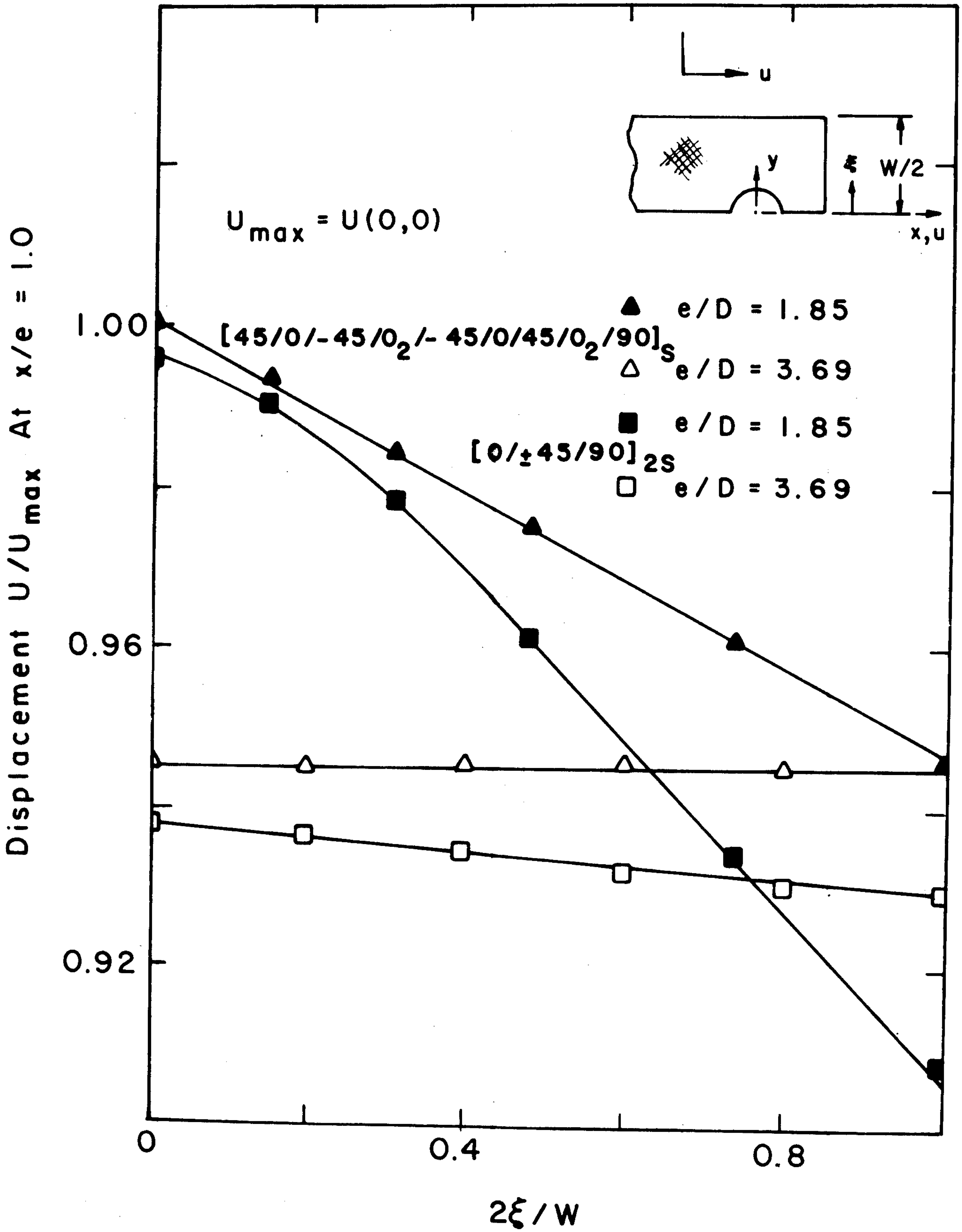

FIGURE 3.7.1 - DEFORMATION OF EDGE UNDER PIN LOADING FOR AS/3501-6 GRAPHITE EPOXY

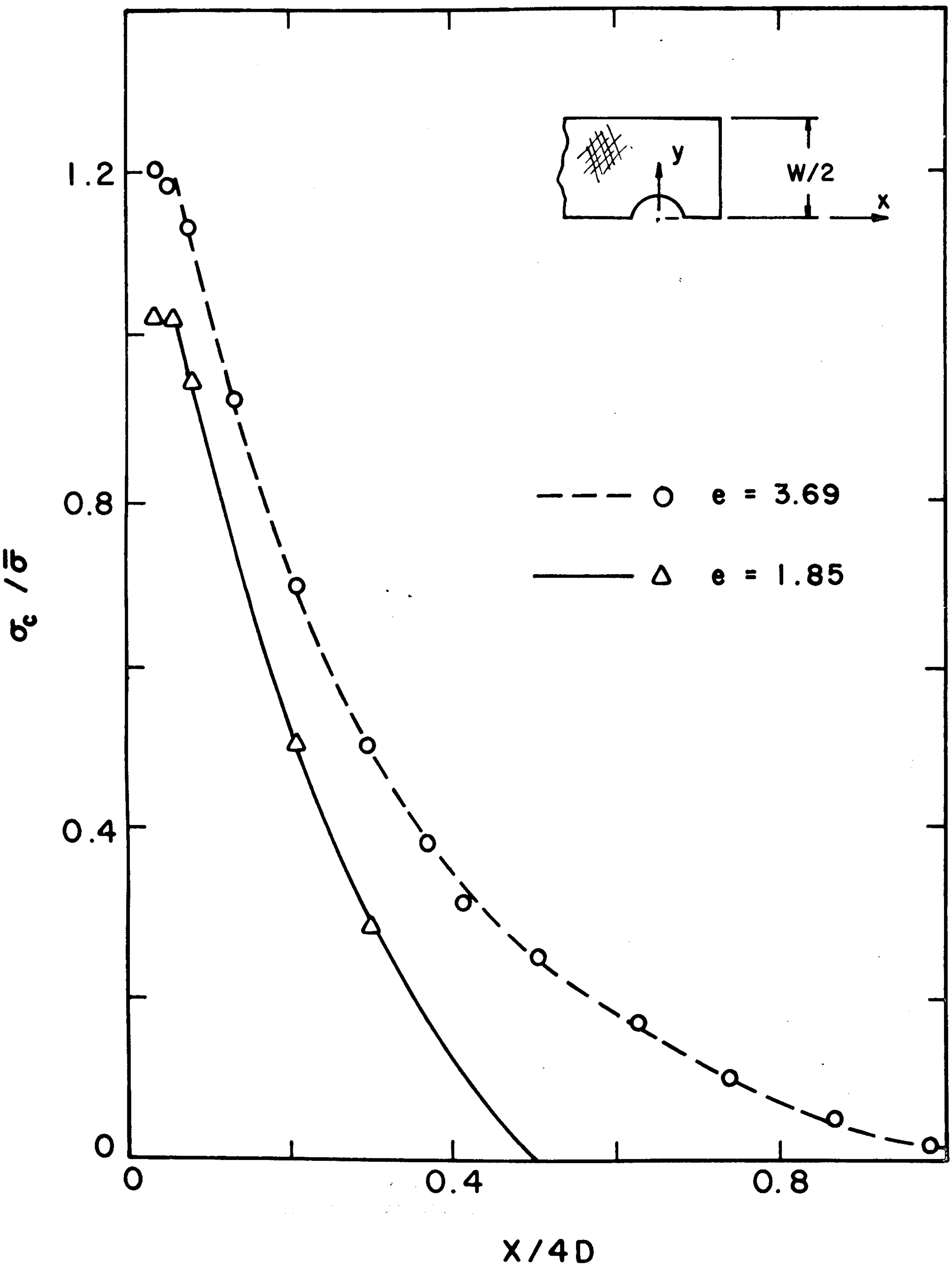

FIGURE 3.8.1 - COMPARISON OF BEARING STRESSES IN QUASI-ISOTROPIC BOLTED JOINT WITH e/D'S OF 1.85 AND 3.69

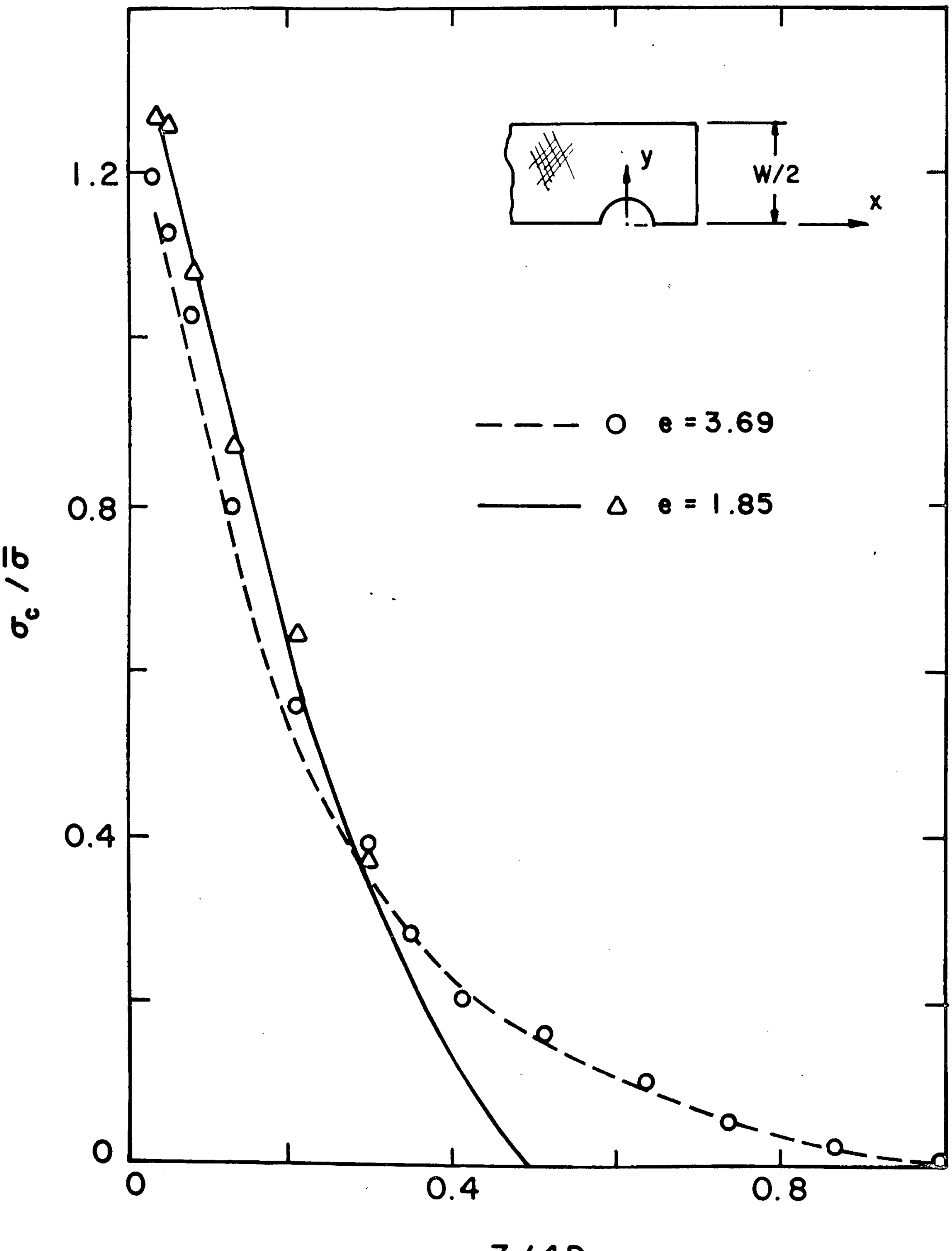

FIGURE 3.8.2 - COMPARISON OF BEARING STRESSES IN 0^{o} DOMINATED BOLTED JOINT WITH e/D'S OF 2 AND 4

COMPOSITE BOLTED JOINT FAILURE MODES

BEARING FAILURE

SHEAROUT FAILURE

COMBINATION SHEAROUT AND NET TENSION FAILURE

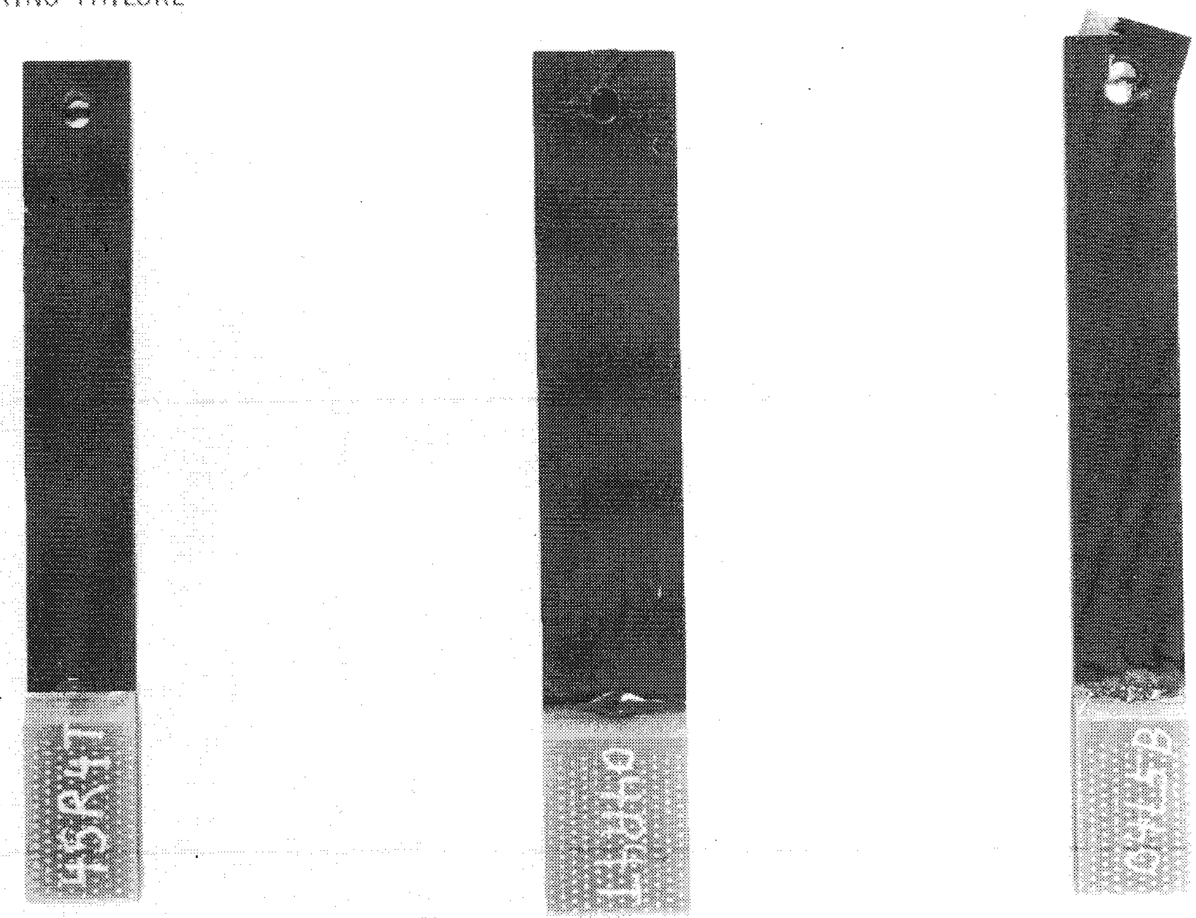

FIGURE 3.9.1 - TYPICAL FAILURE MODES OF THE COUPONS

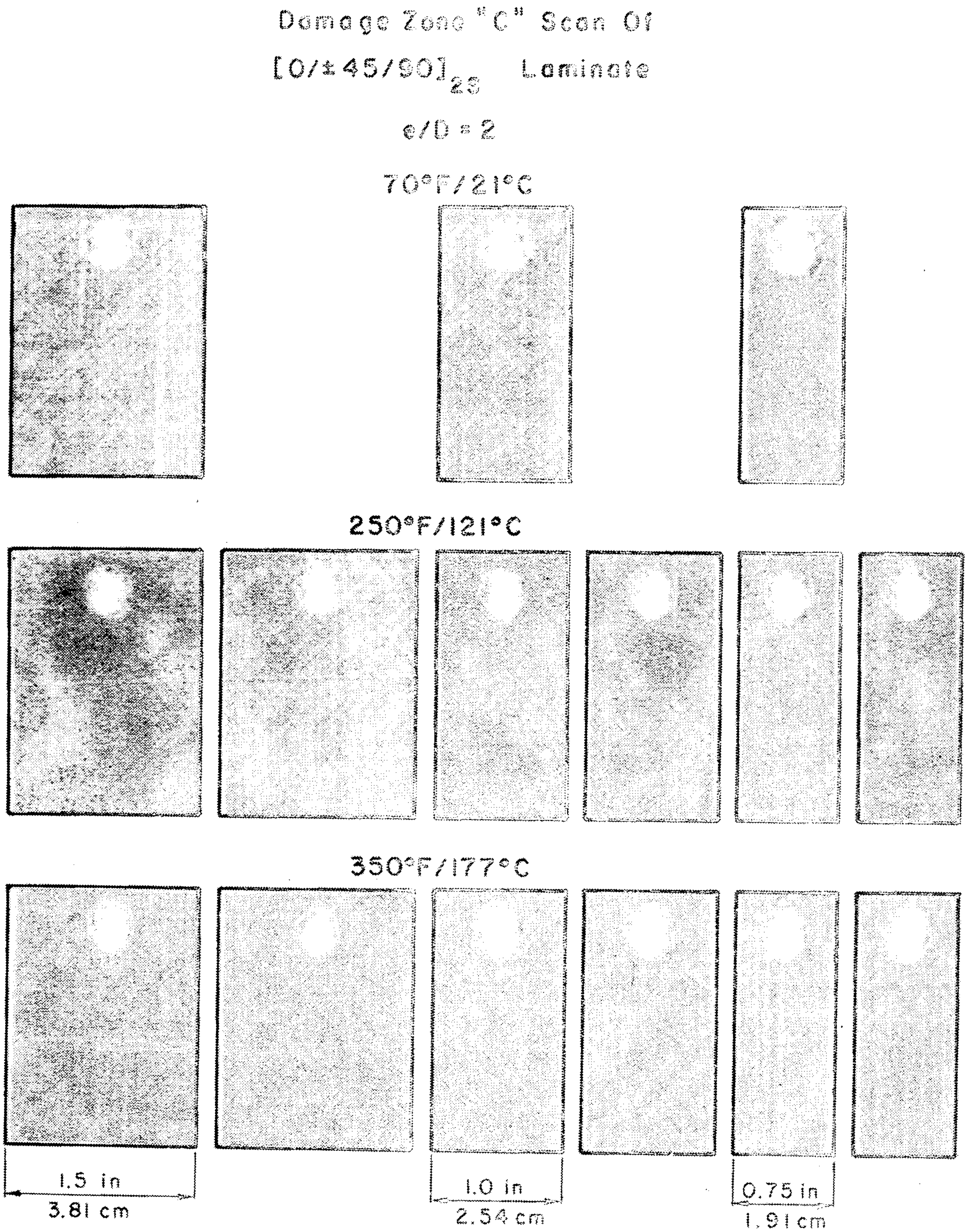

FIGURE 3.9.2 - "C" SCAN OF QUASI-ISOTROPIC COUPONS SHOWING DAMAGE ZONES FOR e/D = 1.85

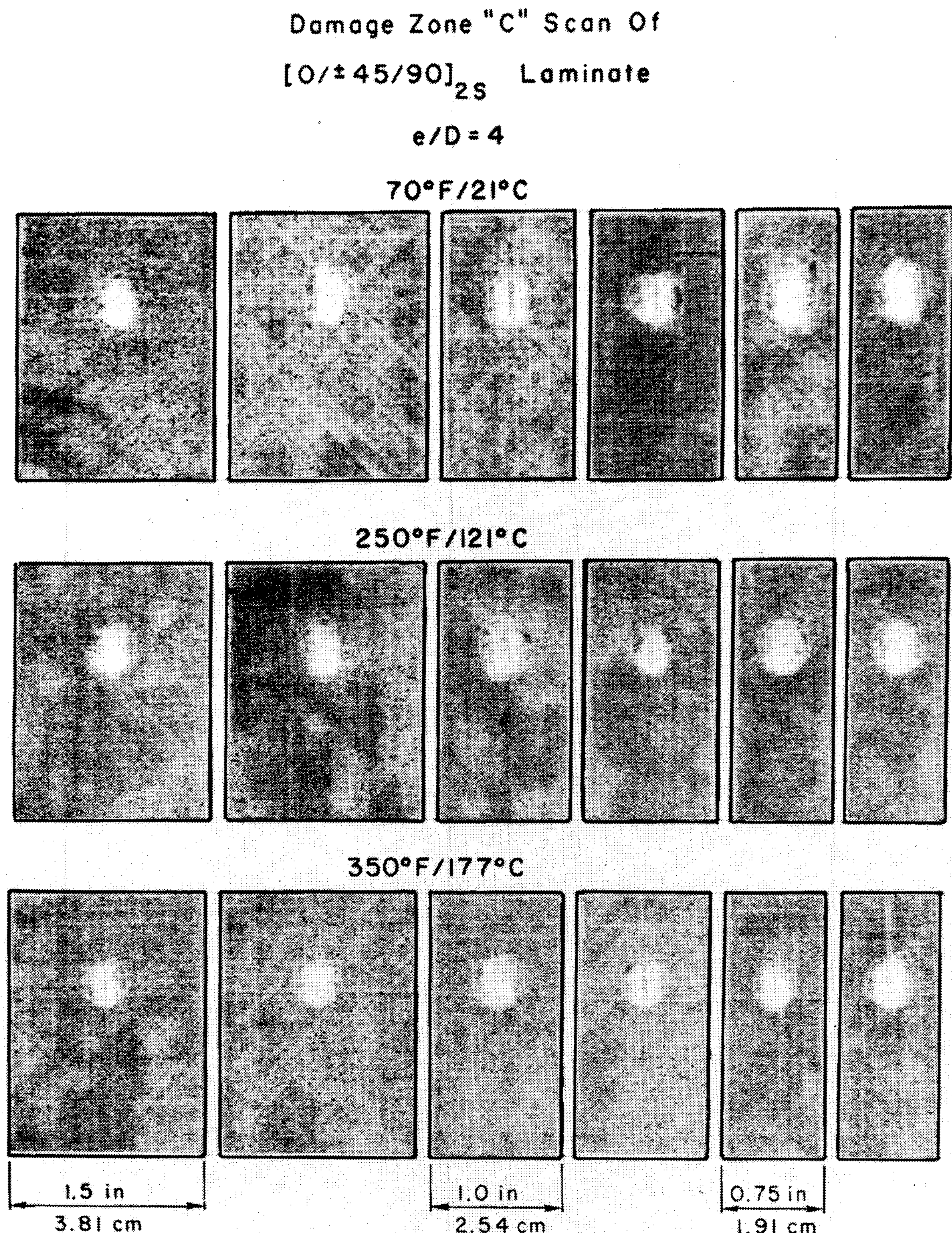

FIGURE 3.9.3 - "C" SCAN OF QUASI-ISOTROPIC COUPONS SHOWING DAMAGE ZONES FOR e/D = 3.69

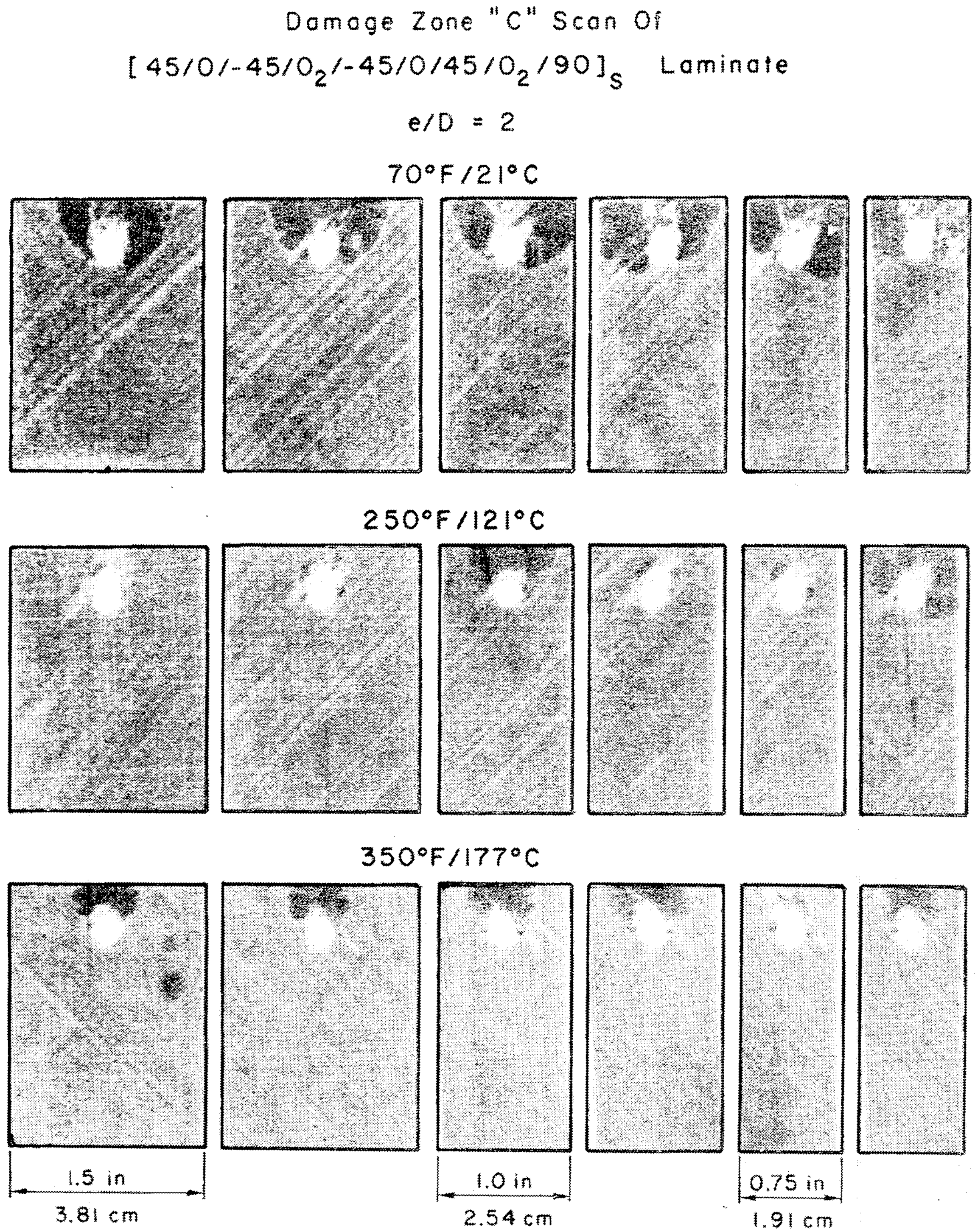

FIGURE 3.9.4 - "C" SCAN OF 0° DOMINATED COUPONS SHOWING DAMAGE ZONES FOR e/D = 1.85

Damage Zone "C" Scan Of

$[45/0/-45/0_2/-45/0/45/0_2/90]_S$ Laminate

$e/D = 4$

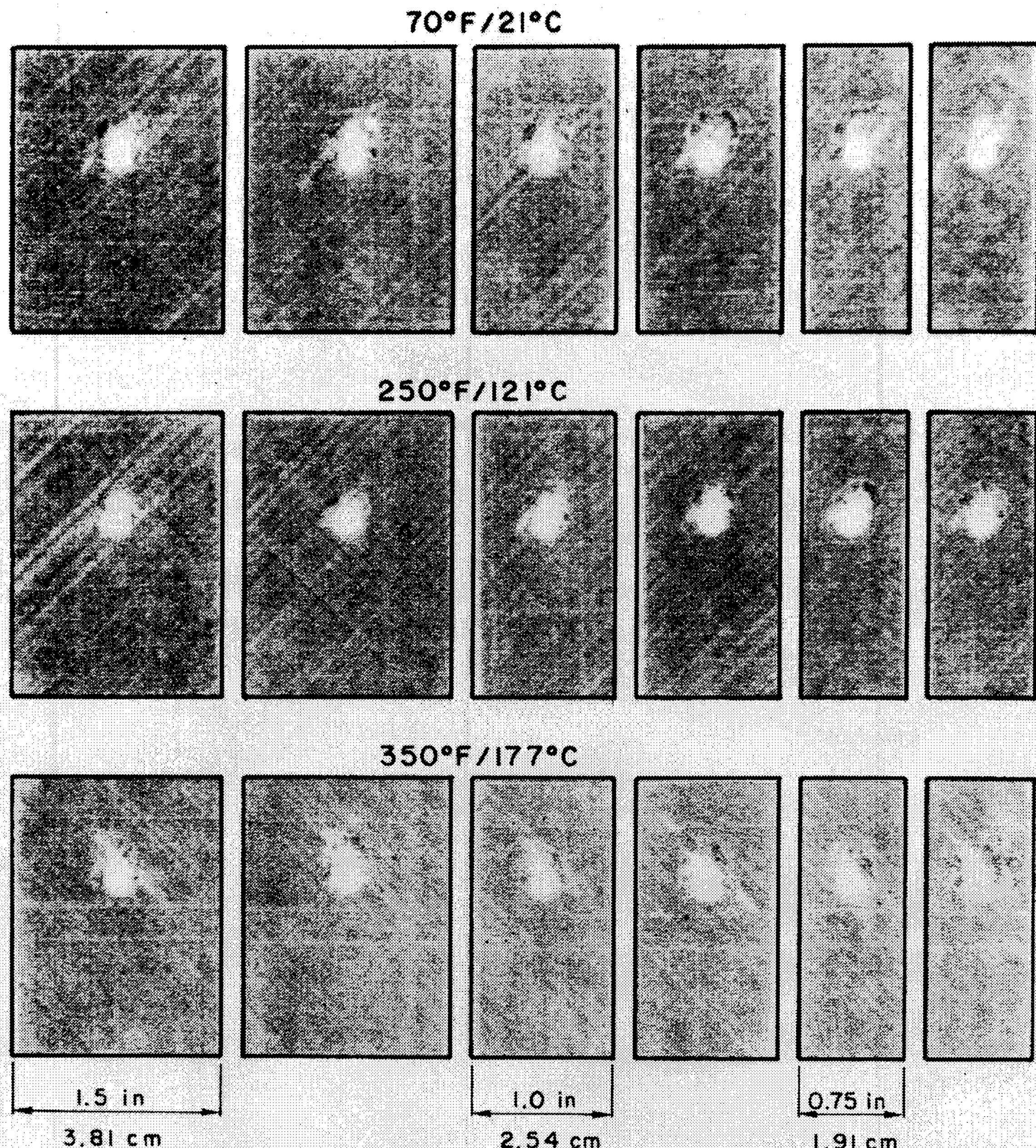

FIGURE 3.9.5 - "C" SCAN OF 0^0 DOMINATED COUPONS SHOWING DAMAGE ZONES FOR $e/D = 3.69$

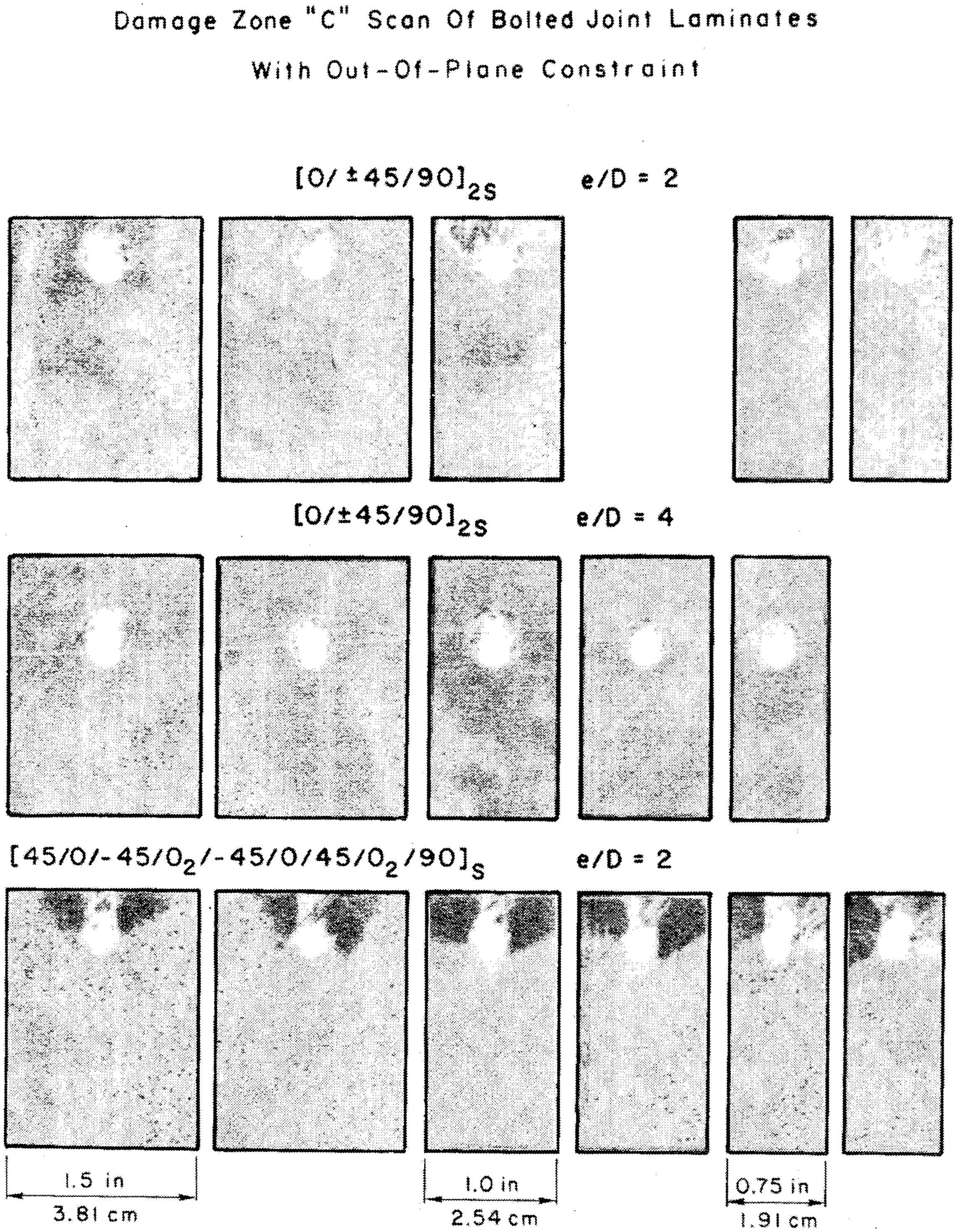

FIGURE 3.9.6 - "C" SCAN OF COUPONS TESTED WITH OUT-OF-PLANE CONSTRAINT

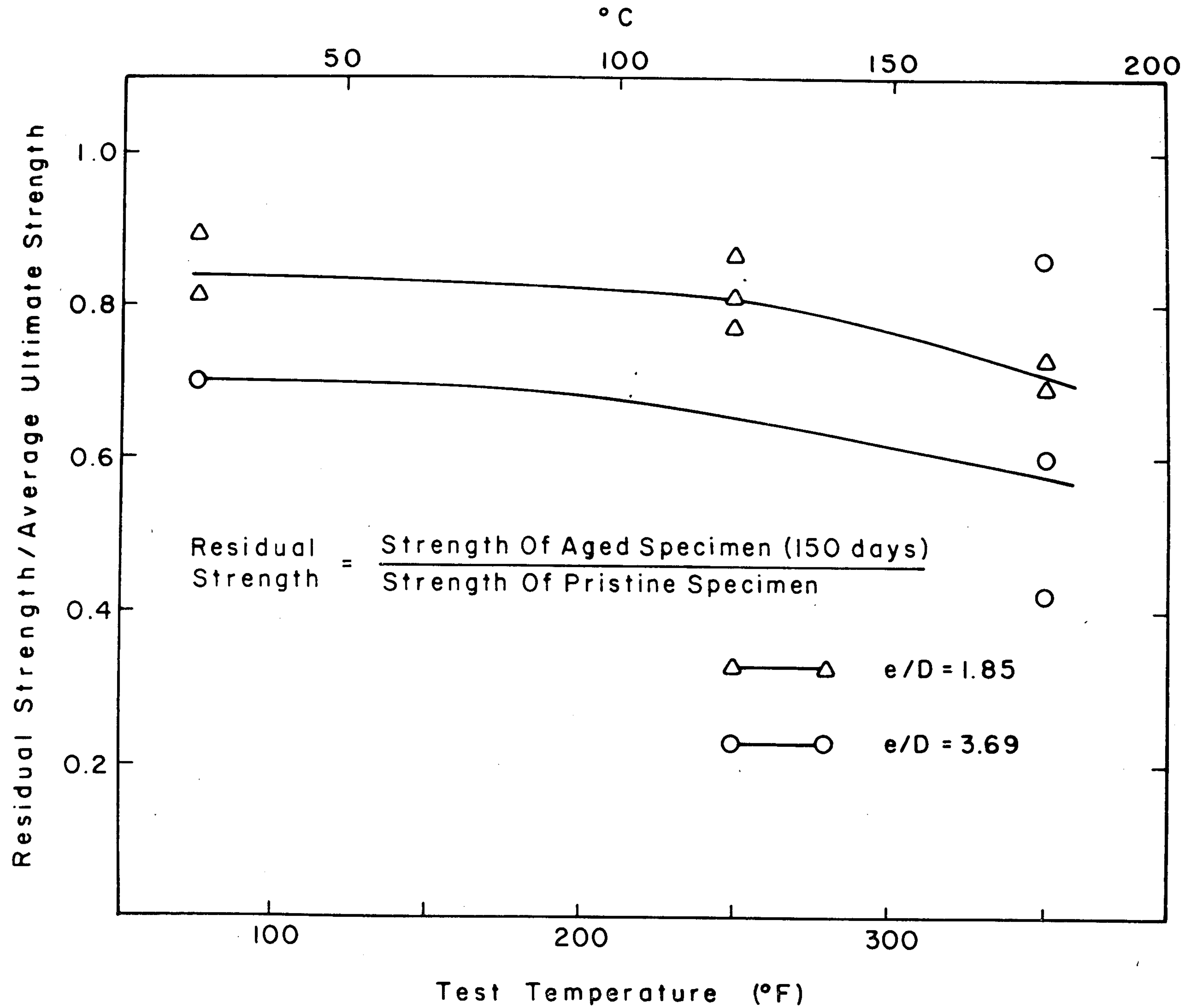

FIGURE 3.10.1 - DECREASED STRENGTH EXHIBITED BY SAMPLES TESTED AFTER 4 MONTH DELAY, QUASI-ISOTROPIC LAMINATE

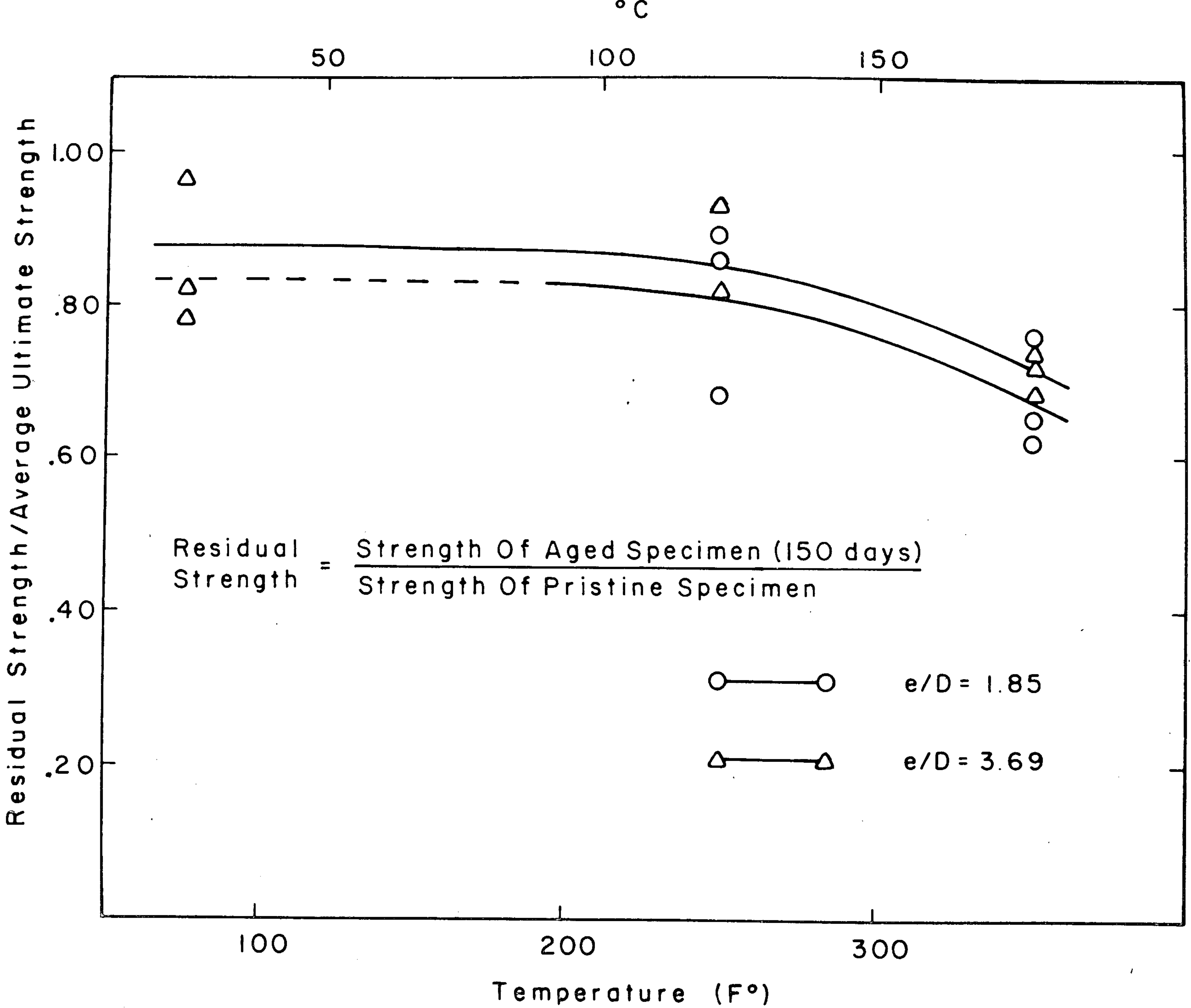

FIGURE 3.10.2 - DECREASED STRENGTH EXHIBITED BY SAMPLES TESTED AFTER 4 MONTH DELAY 0° DOMINATED LAMINATE

1. Report No. NASA CR-159137	2. Government Accession No.	3. Recipient's Catalog No.
4. Title and Subtitle Behavior of Composite Bolted Joints at Elevated Temperature		5. Report Date September 1979
		6. Performing Organization Code
7. Author(s) *Dale W. Wilson and **R. Byron Pipes		8. Performing Organization Report No. CCM-1-78
		10. Work Unit No.
9. Performing Organization Name and Address University of Delaware Center for Composite Materials Newark, Delaware 19711		11. Contract or Grant No. NSG-1409
12. Sponsoring Agency Name and Address National Aeronautics and Space Administration Washington, DC 20546		13. Type of Report and Period Covered Contractor Report
		14. Army Project No.
15. Supplementary Notes *Research Associate **Director Langley Technical Monitor: Dr. Paul A. Cooper		

16. Abstract

Experimental results from an investigation which examines the combined effects of temperature, joint geometry and out-of-plane constraint upon the response of mechanically fastened composite joints are presented. Data are presented for simulated mechanically fastened joint conditions in two laminate configurations ($[0/\pm45/90]_{2s}$ and $[45/0/-45/0_2/-45/0/45/0_2/90]_s$) fabricated from Hercules AS/3501-6 graphite-epoxy. Strength and failure mode results are presented for the test temperatures of 21°C (70°F), 121°C (250°F) and 177°C (350°F) and for a range of the gometric parameters W/D and e/D from 3.71 to 7.43 and 1.85 to 3.69, respectively. A hole diameter, D of 5.16 mm (0.203 in.) was utilized for all tests. Pin bearing tests with out-of-plane constraint were conducted at room temperature only. All elevated temperature data were generated for pin bearing conditions. Three replicates of each test coupon geometry and laminate configuration were tested at each of three temperatures - totalling 126 tests in all. Ultrasonic "C" scan inspection of the failed specimens was employed to assess the damage region and to determine failure mode. Comparative data are presented for pin bearing and out-of-plane constraint conditions for the above mentioned joint configurations. The joint under pin loading was modeled by two-dimensional finite-element methods. Predicted net section strain concentrations were compared with experimental results.

17. Key Words (Suggested by Author(s)) Composite material, Bolted joint, Bearing failure, Shear-out failure, Net tension failure, Ultrasonic "C scan, Graphite epoxy, Finite element methods		18. Distribution Statement Unclassified - Unlimited	
19. Security Classif. (of this report) Unclassified	20. Security Classif. (of this page) Unclassified	21. No. of Pages 104	22. Price* $6.50

*For sale by the National Technical Information Service, Springfield, Virginia 22161